1967

Hydrodynamic lubrication during wire drawing and hyrdostatic extrusion

Arumugam Manoharan
Lehigh University

HYDRODYNAMIC LUBRICATION DURING WIRE DRAWING AND HYDRO-STATIC EXTRUSION

by

Arumugam Manoharan

A Thesis

Presented to the Graduate Faculty

of Lehigh University

in Candidacy for the Degree of

Master of Science

Lehigh University

June 1967

This thesis is accepted and approved in partial fulfillment of the requirements for the degree of Master of Science.

August 10, 1967
date

Betzalel Avitzur
Co-Chairman

Ralph H. Long Jr.
Chairman

Ralph H. Long Jr.
Head of the Department

ACKNOWLEDGEMENTS

The author is indebted to Dr. Betzalel Avitzur of the Metallurgy and Materials Science Department and thesis advisor for his numerous, valuable, constructive and greatly appreciated comments and advice on the various metal forming processes. His counsel and encouragement were invaluable during the course of this work.

Dr. Ralph H. Long, Jr., Chairman of Mechanical Engineering Department is thanked for his valuable comments on lubrication. Mr. William A. Digel is thanked for his editorial work. The Machine Shop of the Metallurgy and Materials Science Department is thanked for its help in preparing the billets for hydrostatic extrusion and samples for tensile testing. Finally, the author wishes to thank the National Science Foundation for its financial support for the work through the Project No. GK-231.

TABLE OF CONTENTS

LIST OF FIGURES

NOMENCLATURE

R_o	Initial radius, outer radius
R_f	Final radius
R	instantaneous radius
m	friction factor
μ	Coulomb friction factor
v	velocity
v_o	original velocity
v_f	final velocity
r, θ, ϕ	axes of spherical coordinate system
r	instantaneous radius in spherical coordinate system
U_r	velocity in 'r' direction
U_θ	velocity in 'θ' direction
U_ϕ	velocity in 'ϕ' direction
Γ	surface of velocity discontinuity
α	semi-cone angle of die
α_{cr}	critical semi-cone angle of die
$f(\alpha)$	a function of α as defined by Eq. (1)
L	length of die land
τ	shear stress
$\bar{\tau}$	average shear stress
h	lubricant film thickness
ε	lubricant film thickness at the exit of die
η	viscosity of lubricant film
S	modified Sommerfeld number

σ_o	yield limit at uniaxial tensile test, also effective flow stress
k	maximum shear stress the material of the billet can withstand.
J^*	the calculated upper bound on power
$\dot{\varepsilon}_{ij}$	components of strain rate tensor
$\dot{\varepsilon}$	strain rate
σ_{xf}	stress exerted on the wire at the exit of the die
σ_{xb}	stress exerted on the wire at the entrance of the die
P_b	pressure at high pressure chamber
P_a	pressure at low pressure chamber
r%	percent reduction in area
T_i	prescribed applied surface fraction
V	volume
$\dot{V}$	volume flow per unit time, volume rate
dv, $\triangle$v	differential volume
A	area
$\triangle$s, ds	differential area
$\dot{W}_i$	internal power of deformation
$\dot{W}_s$	shear power loss
$\dot{W}_f$	power loss due to friction
$\dot{W}_b$	power loss due to application of external forces

DEFINITIONS

Critical (or required) relative lubricant film thickness:

This is the value of the lubricant film thickness required to maintain a continuous lubricant film between die and billet. When the actual value of the lubricant film thickness equals or exceeds this value, hydrodynamic lubrication prevails between die and billet.

Expected relative lubricant film thickness:

This is the value of lubricant film thickness expected to prevail between die and billet for a given set of process variables. When this thickness equals or exceeds the critical relative lubricant film thickness hydrodynamic lubrication prevails between die and billet.

ABSTRACT

Criteria are developed for the existence of hydrodynamic lubrication during hydrostatic extrusion and wire drawing. For hydrostatic extrusion the criterion is given in terms of the friction factor and the minimum lubricant film thickness required to maintain a complete separation between the die and billet. The critical cone angle of the die below which hydrodynamic lubrication will prevail is predicted for any percent reduction of area.

In wire drawing, the exit velocity of the wire necessary to maintain hydrodynamic lubrication is predicted for any percent reduction of area. The critical velocity is defined in terms of the minimum lubricant film thickness required to maintain a complete separation between the die and the wire.

Drill rod billets were hydrostatically extruded with and without hydrodynamic lubrication, and the results were consistant with the theory developed.

INTRODUCTION

WIRE DRAWING:

When a wire of initial radius R_o is pulled through the conical portion of a die to a final radius R_f, the process is called wire drawing (see Fig. 1). The cylindrical portion of the die, which is called the land, causes frictional losses but is required for dimensional stability and because of die manufacturing practice. The plastic flow to accomplish the desired change in shape is caused by compressive forces set up by the reaction of the metal with the die.

The process, equipment, effect of friction, back pull, reduction, etc., on the drawing force are described in Ref. 22.

Assuming a kinematically admissible velocity field (Fig. 2; described on page 4), Avitzur (2)* derived expressions for the relative drawing stress and maximum possible reduction, using the upper bound method. To simplify the computations, he also made the following assumptions:

(1) The die is a rigid body of the geometry shown in Fig. 1.

(2) The wire is a Mises' material (obeying Mises' stress-strain rate law), which implies no strain hardening effect and no elastic deformations, and consequently no volumetric change.

(3) For the upperbound on energies, the contact surface

---

*Numbers in brackets designate references listed on Page 73 .

between the die and wire is a surface of velocity discontinuity.

He derived the expressions separately for both the assumptions of constant friction factor (m) and Coulomb friction (μ) between die and wire.

He concluded that:

(1) The drawing forces are linearly proportional to the yield stress of the wire.

(2) Increases in reduction, coefficient of friction, and die land all cause an increase in the drawing force.

(3) For any combination of reduction and coefficient of friction there exists an optimum cone angle which minimizes the drawing force.

(4) The die land does not affect the maximum possible reduction when Coulomb friction is assumed between die and billet.

(5) Speed is not a factor in the calculation of the required drawing force when hydrodynamic lubrication (described on page 13) is not prevailing between the die and billet.

Wistreich (1) studied the relations between external forces and process parameters. Using dies split in half longitudinally, he measured the drawing force, mean die pressure, and the mean coefficient of friction. He found his results in good accord with Siebel's theory. His work is described in detail in Ref. 1. Avitzur has compared his theory with Wistreich's experimental results in Ref. 3.

Avitzur's kinematically admissible velocity field:

In order to use the upper bound theorem, a kinematically admissible strain rate field is necessary. This can be derived from a kinematically admissible velocity field. A velocity field is admissible if the velocity components and their first derivatives are continuous except at allowable surfaces of velocity discontinuity, the sum of the normal components of the strains and the sum of the normal components of the strain rates are zero (incompressibility), and the geometric boundary conditions are met. Surfaces of velocity discontinuity are allowable when the normal velocity components on either side of the surface are equal in magnitude and direction. Figure 2 shows a kinematically admissible velocity field proposed by Avitzur (2).

Assuming that the die is a rigid body, the billet is divided into three regions in which the velocity field is continuous. The uniform velocity in zones I and III has an axial component only. In zone I the velocity is v_o and in zone III it is v_f.

Due to volume constancy,

$$v_o = v_f \left(\frac{R_f}{R_o}\right)^2 \qquad \text{(I)}$$

The velocity in the deformation zone II is directed towards the apex of the cone, o. In a spherical coordinate system (r, θ and ϕ) the velocity components are,

$$U_r = v = - V_f r_f^2 \frac{\cos \theta}{r^2}$$

$$U_\theta = U_\phi = 0 \qquad \text{(II)}$$

This is Eq. (12) of Ref. 2.

Across the boundaries Γ_1 and Γ_2, the components of velocity normal to the surfaces Γ_1 and Γ_2 are continuous. But there exist velocity discontinuities parallel to the surfaces, of magnitudes $v_f \sin \theta$ and $v_o \sin \theta$ along Γ_1 and Γ_2 respectively.

Since the die is at rest, the velocity discontinuity is $v_f r_f^2 \frac{\cos \alpha}{r^2}$ parallel to the surface Γ_3 and v_f along Γ_4. No velocity components exist normal to surfaces Γ_3 and Γ_4 and hence there is no velocity discontinuity normal to the surface.

EXTRUSION:

Extrusion is a process whereby a block of solid metal is converted into a continuous length of uniform cross section by forcing it to flow under high pressure through a die orifice which is shaped to impart the required form to the product. Basically there are 3 types of extrusion (see Fig. 3), direct, indirect and impact.

A detailed description of the process and the various effects of the process variables on the process are presented in Ref. 10. Pearson and Parkins (6) explain the process and equipment for extrusion of soft and hard metals.

Assuming a kinematically admissible velocity field, Avitzur (7) has computed the power and derived an expression for extrusion stress using the upper bound approach. His conclusions for square die design (details given on page 7) are:

Beginning of stroke:

(1) The dead zone angle and the extrusion stress increase with the extrusion ratio in direct and indirect extrusion.

(2) The dead zone angle decreases in direct extrusion with increasing friction and increases in indirect extrusion. The extrusion stress increases with friction.

(3) The extrusion stress increases when longer billets are used in direct extrusion, while it is unaffected in indirect extrusion. The dead zone angle is unaffected.

End of stroke:

(1) The inner pipe (explained on page 7) radius increases with decreasing extrusion ratio with increasing friction and with decreasing billet length.

(2) The extrusion stress increases with extrusion ratio and friction.

(3) The critical length when piping sets in decreases with increasing extrusion ratio and with decreasing friction.

(4) As billet length decreases, the extrusion stress passes through a minimum.

Frisch and Thomsen (8) studied the effect of the process variables on extrusion pressures for lead. Their conclusions are:

(1) With good lubrication and good cylinder wall finish, the extrusion pressures for 2 in. dia. x 3 in. long commercially pure lead billets are essentially identical for both direct and indirect extrusion when extruded at room temperature and with an extrusion ratio $\frac{R_o}{R_f}$ of 8·4.

(2) Eccentricity of a single bar or as many as three bars (see Figs. 2 and 3 of Ref. 8) extruded at the same

ratio does not appear to influence the extrusion pressure.

(3) For 4.3 in. and 2.0 in. dia. billets, the extrusion pressures appear to be influenced very little by size effect for the same extrusion ratios.

(4) Extrusion pressures for a wide range of extrusion speeds investigated were approximately linear when plotted on log log coordinates.

Piping defect:

A well-known defect in extrusion is cavity formation at the center on the back of the billet, a process which begins when the billet becomes relatively short. The cavity gradually increases in diameter and depth, transforming the emerging rod into a pipe of increasing inner diameter, with the result that the product has to be discarded. This defect can be reduced or eliminated if dies of smaller cone angles are used. More details on this defect can be found in Ref. 7

Square die:

A die with $\alpha = 90°$ is known as a square die. When square dies are used a dead zone is always formed, and the dead zone metal acts as the die. Since the optimum cone angle increases with the die angle, the friction losses are higher with square dies.

The advantages with square dies are: 1) it is easy to manufacture them and 2) the wear on the die is much less because of the dead zone formation.

However, in industry, dies with less than 90°(α) are widely used (10), a common die angle being 63°(α). Experiments on En 2A

steel with extrusion ratios of 4.0 and 1.79 (Ref. 10) showed that the maximum extrusion pressure decreased as the semi-cone angle (α) decreased from 90°(square die) to 30° and then remained constant for a further reduction to 20°.

Also, with conical dies, during hot extrusion a state of hydrodynamic lubrication (which is the subject matter of this thesis) exists when glass is used as the lubricant. Details are given on page 16.

Hydrostatic extrusion:

Hydrostatic extrusion, known also as ramless, fluid, hydraulic extrusion, is a new process. Unlike the well-established processes of direct and indirect extrusion, the external force in this process is tranferred to the free-surface of the billet by means of a liquid under pressure, instead of by direct contact with a ram (Fig. 4). Pressure at the die orifice is lower than that at the die entrance and the resulting pressure differential causes metal flow.

In ram extrusion, the friction losses are higher because the billet is in contact with the die, the extrusion chamber, and the ram. In hydrostatic extrusion the billet is in contact with the die only. The absence of contact between billet and chamber means that the billet-chamber friction is virtually eliminated and consequently the extrusion pressure can be expected to be lower than that for conventional extrusion under comparable conditions. Also, the extrusion pressure is almost unaffected by the length of the billet. In addition, because of the support given by the liquid to the sides of the billet, long billets of any shape, such as coils of wire, can

be extruded without buckling and without any increase in the extrusion pressure (16).

Bobrowsky and Stack (19) hydrostatically extruded 0.375 in. dia. billets of 3S aluminum through a die of 0.300 in. exit dia. The percent reduction was 90%. The extrusion and receiver pressures were 350,000 psi and 250,000 psi, respectively.

Considerable investigation of hydrostatic extrusion has been performed at the National Engineering Laboratory (NEL) in Glasgow, Scotland. The details, such as the process, equipment, estimation of pressure required, the effect of process variables on the extrusion pressure, the properties of extruded products, etc., are described in Ref. 16.

Assuming the kinematically admissible velocity field, explained on page 4 , Avitzur (18) has derived expressions for the pressure required for hydrostatic extrusion in terms of the process variables using the upper bound method. He conducted experiments on commerical lead (99.7% pure). The following die semi-cone angles were used: 10°, 15°, 20°, 30°, 45°, 60°, 75° and 90°. The following reductions of area were tried: 25%, 45%, 60%, 70% and 80%. The results are given in Ref. 19.

Hillier (30) studied the possibility of hydrodynamic lubrication in hydrostatic extrusion.

The work done at the Metalworking Research Division of the Battelle Memorial Institute is described in Ref. 14.

FRICTION AND LUBRICATION:

Modern friction theory is based on the premise that real surfaces are not smooth, but have an inherent roughness or texture. Bowden and Tabor (20) describe the measurement of the contour of real surfaces by the following methods: (1) profilometer, (2) optical interference methods, (3) electron microscopy, and (4) electron diffraction. When two such surfaces come into contact, they are supported on a very small portion of the apparent contact area (Fig. 5) and the resulting unit pressures at the contacting asperities are very high even under light loads. Elastic and plastic deformation and welding of asperities occur. The friction force is presumed to be the force necessary to shear the junctions formed at the asperities.

Amonton's Law, i.e., frictional resistance is proportional to the load and independent of the area of contract, is usually followed (22). A generally accepted version of Amonton's Law is:

$$F = \frac{WS}{p}$$ where F = Frictional force

W = load

S = shear strength of junction

p = compressive yield stress of the asperities.

Amonton's law is far from universal and many examples of deviation from it can be given, for instance, the friction of steel on ice and steel on Teflon where friction force decreases with load under certain conditions. Deviations from Amonton's law are prevalent in metal deformation processes.

Bowden and Tabor recognized three factors as significant in causing resistence to sliding: (1) shearing of asperity contact junctions, (2) ploughing of hard asperities through a softer surface with which they are in contact. Ploughing is most significant only when one surface is much harder than the other, as in abrasion by hard particles, filing of surfaces, and various metal deformation processes, (3) ploughing due to foreign hard particles such as worn out particles from the parent material, oxides and other surface contaminations like hydrocarbon, resins, etc.

The initial shearing within asperity contacts increases the true area of contact, brings the surfaces closer, and presumably brings more asperities into contact (22). The resulting increase in contact area will limit the amount of plastic deformation of asperities because of the reduction of contact stress. Work hardening of the asperities further reduces the tendency for plastic flow in the asperity junctions and as "wear in" continues, deformation becomes predominantly elastic.

As noted earlier, in general, Amonton's law is not obeyed during such metal deformation processes as forging, extrusion, and upsetting. Instead, the coefficient of friction decreases with increasing load after bulk flow begins in the work piece. Where provisions have been made to measure interfacial shear forces during metal deformation, friction-contact stress characteristics similar to those shown in Fig. 6 (Fig. 12 of Ref. 22) have been observed. It is clear from the figure that Amonton's law is not obeyed in metal deformation processes.

The coefficient of friction gives a measure of friction between

the surfaces. Wistreich (1) describes a method of measuring the coefficient of friction by using split dies in wire drawing. Avitzur describes in Ref. 35 an experimental procedure for the measurement of average friction in wire drawing, open die extrusion, and hydrostatic extrusion.

To reduce the friction and thus reduce the wear between the rubbing surfaces and also to dissipate the heat generated because of the relative motion, a lubricating fluid is introduced between the surfaces. The lubricants are basically petroleum products. The effectiveness of the lubricant depends on its properties, such as cohesiveness, adhesiveness, and viscosity, of which viscosity is the most important. Hersey (26) and Davis (23) describe methods of measuring viscosity of lubricants. Hersey (26) and Tipei (28) describe the variation of viscosity with pressure and temperature.

When there is a lubricant film between the sliding surfaces, the friction is either semi-fluid (boundary lubrication) or fluid (hydrodynamic lubrication).

When the sliding surfaces are separated by lubricant films only a few molecules in thickness, boundary lubrication exists. It prevails when the load between the surfaces is high and the relative speed is very low. When boundary lubrication prevails, the friction is influenced by the nature of the underlying surface as well as the chemical constitution of the lubricant. Viscosity plays little or no part in the frictional behavior in boundary lubrication (20).

The load is supported both by the lubricant film and by minute

metallic junctions formed through the lubricant film. Thus the frictional force may be expressed as the sum of two terms (20); (1) the force required to shear the metallic junctions, and (2) the force required to shear the lubricant film. The metallic pick up is considerably reduced. But the reduction in friction is much less than the reduction in metallic pick up.

When the sliding surfaces are completely separated by a continuous film of lubricant, the resistance to the motion arises solely from the viscosity of the lubricant (20). This type of lubrication, called hydrodynamic lubrication, prevails when the load between the moving surfaces is relatively low and both the viscosity of lubricant and the relative speed are high. When hydrodynamic lubrication prevails, the friction is less and the wear on the surfaces is almost nil.

Sommerfeld (24), Clower (27), and Bowden and Tabor (20) discuss hydrodynamic lubrication in a journal bearing.

Bowden and Tabor (20) show that the distance of nearest approach between the surfaces depends on a parameter of the type $\frac{ZN}{p}$ (Z = viscosity, N = speed in RPM, p = load). Consequently, when the viscosity or speed is low or if the load is high, the theoretical separation of the surface may be less than the height of the surface asperities. The surfaces are no longer separated completely by the lubricant film. The asperities will rub on one another and will be separated by no more than one or two molecular layers of lubricant. This is the previously mentioned boundary lubrication under which some wear may occur.

Stribeck (21) plotted the coefficient of friction against the parameter $\frac{ZN}{p}$ for a journal bearing (Fig. 7). The lowest point of the curve represents the point where complete separation of the journal and bearing has occurred and consequently the coefficient of friction is the lowest. Beyond that point, for higher values of N (assuming Z and p constant) the fluid film thickness is greater and the coefficient of friction is higher because of an increase in shearing of fluid film. Conversely, if N is reduced, less lubricant is drawn between the surfaces and the surfaces are no longer completely separated by the lubricant. Metallic contact is beginning to occur, and only a partial fluid film can be maintained. This is mixed friction region. The friction here is a function of fluid shear and metal contact. Consequently, the coefficient of friction is higher. If the speed is reduced still further, another region results where a fluid film cannot be maintained. This is where boundary lubrication prevails.

Figure 7 can also be plotted for $\frac{\bar{\tau}}{\sigma}$ vs $\frac{\eta V_f}{\sigma_o R_f}$ for metal deformation processes like wire drawing, extrusion, and hydrostatic extrusion. Assuming η, σ_o, and R_f to be constant, it will show the variation of exit velocity with the relative shearing stress at the conical surface of contact between the die and billet. As the exit velocity exceeds a particular value, hydrodynamic lubrication exists between the die and billet, and below that value boundary and mixed lubrication exist, depending on the value of exit velocity.

In recent years, several researchers have explored the application of hydrodynamic lubrication to wire drawing. Christopherson (31) studied the conditions under which hydrodynamic lubrication will occur in wire drawing. He used a relatively long tube (60 to 500 wire diameter) that had a diameter only slightly larger than the wire at the entrance to the die (Fig. 8). The tube was firmly attached to the die. The lubricant was supplied to the wire, adhered to the wire surface, and was drawn into the tube by its viscosity. As the wire travelled through the tube at a high velocity, pressures up to 40,000 psi were developed at a speed of 600 ft/min. Higher drawing speeds could increase the pressure of the lubricant.

The main practical obstacle is that hydrodynamic conditions at the entrance of the die are induced by high drawing speeds and do not operate during stopping and starting of drawing. There also has been resistance in the wire drawing industry to the use of rather long tubes with the small clearances required in front of the die.

Moseev and Korostelin (33) and Butler (34) studied the possibility of obtaining hydrodynamic lubrication conditions by pressurizing the lubricant with an external hydraulic pump. Their studies indicate that this method makes the fluid pressure applied to the die controllable and independent of fluid viscosity, drawing speed, and process geometry. The method was successfully used in tests at drawing speeds up to nearly 1000 ft/min. for singlepass reductions of 30 to 35 percent. This method might be used to best advantage for the continuous drawing of wire, since the system must be depressurized before the tail end of the wire enters the first (ironing) die.

Figure 9 (Fig. 20 of Ref. 29) shows the cross section of a patented nozzle-die unit developed at the Sheffield Laboratories of the British Iron and Steel Research Association (BISRA) in which dry powdered soap is used as the lubricant (32). The wire passes through the tube, which has a tungsten carbide liner, and then into the die where it is reduced in diameter. Powdered soap is carried by the moving wire from the soap box to the bell-shaped opening of the nozzle where it is compacted and then liquified in the parallel portion of the nozzle. The movement of the wire causes the pressure to increase rapidly along the tube to about 60,000 psi at the die entry. This high pressure causes a greatly increased flow of soap through the die so that the quantity of soap lubricant on the drawn wire may be 70 to 80 times greater than in normal dry drawing. In a multiple drawing machine the nozzle is generally fitted only on the first die and the amount of soap used is only slightly greater than that required for normal dry soap drawing of wire. The thicker film of soap on the wire significantly improves the lubrication in all the subsequent dies of a multidraw machine. Industrial trials with these nozzles resulted in 3 to 8 times longer die life (32). The apparent disadvantage is the less efficient lubrication because of reduced speed while starting and stopping the drawing operation.

It has been proved (37) that hydrodynamic lubrication exists during conventional hot extrusion with conical dies when glass is used as the lubricant. The billet is rolled in powdered glass and a glass/silicate pad is put into the die to provide a continuous supply of glass as needed during extrusion. At the high extrusion tempera-

ture, the glass melts and forms a uniform layer between the die and billet and keeps them completely separated (hydrodynamic lubrication).

Glass as a lubricant has the following advantages over graphite (another common lubricant):

(1) it acts as an insulator, preventing the billets from being severely chilled when they come into contact with the tools. This in turn helps to avoid transverse breaks on the surface of the extruded product.

(2) Because of the insulation that glass gives the tools, they last longer.

(3) Thinner and smaller diameter tubes can be made (in tube extruding), i.e., greater extrusion ratios are possible.

(4) It is clean in working.

(5) No carbon pick up occurs.

(6) It is viscous at the working temperature and therefore keeps feeding through the die, which means that very long extrusions can be made. Heavier billets can be used, thus increasing the yield.

(7) It has made the extrusion of sections and hollow shapes with comparatively sharp corners practicable on a production basis.

Some of the disadvantages of glass compared with graphite are:

(1) It is more expensive.

(2) It is more difficult to remove from the surface of the product.

(3) The surface finish of the billet has to be very good, since the glass keeps the metal surface and die surface apart and any surface roughness on the billet is unchanged.

(4) The billets must be, practically speaking, free from scale; otherwise, the extruded products will have much poorer surfaces than if graphite had been used.

It is obvious from the above that if hydrodynamic lubrication can be predictable in any metal forming process, it will result in a considerable saving in power required for the process and also longer tool life.

It is the purpose of this thesis to develop criteria for the existence of hydrodynamic lubrication during hydrostatic extrusion and wire drawing in terms of the process variables. This study is an extension of the derivation presented for hydrodynamic lubrication in Ref. 35.

It will be assumed that the material being drawn or extruded is an incompressible Mises' material which does not strain harden. The die profile is conical and the problem considered is one of axial symmetry. The lubricant fluid film thickness is small compared with the diameter of the wire or billet. Liquid flow in the lubricant film is assumed to be laminar, viscous, and Newtonian.

RESULTS

For hydrostatic extrusion, the critical semi-cone angle, α_{CR}, below which hydrodynamic lubrication will prevail, is

$$\alpha_{CR} = \cot^{-1}\left\{\frac{2\sqrt{3}\,(\varepsilon/R_f)\,f(\alpha)}{m\,\ln\left(\frac{R_o}{R_f}\right)}\left[\frac{1.5\,(\varepsilon/R_f)}{\left(\frac{R_o}{R_f}\right)^3-1}+1\right]\right\} \qquad (1)$$

for $L=0$

when $L\neq 0$, α_{CR} can be found from the following equation:

$$\left[\cot\alpha_{CR}\ln\left(\frac{R_o}{R_f}\right)+\frac{L}{R_f}\right]=\frac{\sqrt{3}}{m}f(\alpha)\left(\frac{\varepsilon}{R_f}\right)\left[2+\frac{(\varepsilon/R_f)\left\langle\cot\alpha_{CR}\cos^2\alpha_{CR}\left(\frac{R_f}{R_o}\right)^3+\frac{L}{R_f}\right\rangle}{\left\langle\frac{\cot\alpha_{CR}\cos^2\alpha_{CR}}{3}\left[1-\left(\frac{R_f}{R_o}\right)^3\right]+\frac{L}{R_f}\right\rangle}\right]$$

where $$\frac{\varepsilon}{R_f}=\sqrt{\frac{V_f\eta}{R_f\sigma_o}\,\frac{1}{f(\alpha)}\left\langle\frac{\cot\alpha\cos^2\alpha}{3}\left[1-\left(\frac{R_f}{R_o}\right)^3\right]+\frac{L}{R_f}\right\rangle} \qquad (1a)$$

and $$f(\alpha)=\frac{1}{\sin^2\alpha}\left\{1-\cos\alpha\sqrt{1-\tfrac{11}{12}\sin^2\alpha}+\frac{1}{\sqrt{11\cdot 12}}\ln\frac{1+\sqrt{\frac{11}{12}}}{\sqrt{\frac{11}{12}}\cos\alpha+\sqrt{1-\frac{11}{12}\sin^2\alpha}}\right\}$$

Equation (1) is plotted in Fig. 11. For $\frac{R_o}{R_f}=2$ and $L=0$, Fig. 11 represents the effect of relative lubricant film thickness and friction factor on the critical die semi-cone angle. For any value of friction factor and relative lubricant film thickness, the critical die cone angle can be read from Fig. 11.

It can be seen from Fig. 11 that, as the friction factor increases, the critical die semi-cone angle increases sharply. For very low values of relative lubricant film thickness $\frac{\varepsilon}{R_f}$, α_{CR} increases rapidly and then remains practically constant for all values of friction factor.

For wire drawing, hydrodynamic lubrication is predicted from the following equation:

$$\left(\frac{\varepsilon}{R_f}\right) = \sqrt{\frac{S}{f(\alpha)}\left\langle \frac{\cot\alpha\,\cos^2\alpha}{3}\left[1-\left(\frac{R_f}{R_o}\right)^3\right] + \frac{L}{R_f}\right\rangle} \qquad (2)$$

where $S = \dfrac{V_f \eta}{R_f \sigma_o}$

Equation (2) is plotted in Figs. 12 and 13. For $\frac{L}{R_f} = 0.2$ and r = 25%, Figs. 12 and 13 represent the effect of $\frac{\varepsilon}{R_f}$ and α on the critical exit velocity of wire. Referring to Figs. 12 and 13, it is seen that, for a constant value of relative lubricant film thickness $\frac{\varepsilon}{R_f}$, the critical exit velocity above which hydrodynamic lubrication will prevail increases sharply as the semi-cone angle of the die increases. In other words, to maintain hydrodynamic lubrication, the exit velocity of the wire has to be increased considerably as the semi-cone angle of the die is increased.

Also, it is seen from Figs. 12 and 13 that as the relative lubricant film thickness is increased, the critical exit velocity required to maintain it also increases for a constant semi-cone angle of the die.

When the value of the lubricant film thickness to be maintained is known, the region above the line corresponding to that value of $\frac{\varepsilon}{R_f}$ represents the region where hydrodynamic lubrication will prevail. Any velocity in that region will maintain hydrodynamic lubrication with that value of lubricant film thickness.

DERIVATION

Hydrodynamic lubrication is assumed to prevail between the die and the billet. The drawing stress required to draw the billet through the die is derived using the upper bound theorem.

In suggesting that limit analysis should be a powerful tool for the analysis of plastic deformation of metals, Prager and Hodge (36) have formulated an upper bound theorem. They state that among all kinematically admissible strain rate fields the actual one minimizes the expression

$$J^* = \sqrt{2}\, k \int_V \sqrt{\dot{\varepsilon}_{ij}\, \dot{\varepsilon}_{ij}}\, dV - \int_S T_i\, v_i\, ds \qquad (4)$$

where J* is the calculated upper bound on power. If von Mises' yield criterion is assumed, the maximum shear stress, k, that a material can stand will be given by the equation $k = \frac{\sigma_0}{\sqrt{3}}$.

Thus, assuming the stress strain relationship of von Mises, Eq. (4) becomes

$$J^* = \frac{2}{\sqrt{3}}\, \sigma_0 \int_V \sqrt{\tfrac{1}{2}\, \dot{\varepsilon}_{ij}\, \dot{\varepsilon}_{ij}}\, dV - \int_S T_i\, v_i\, ds \qquad (5)$$

If surfaces of velocity discontinuities are to be included, the upper bound equation may now be written as

$$J^* = \frac{2}{\sqrt{3}}\, \sigma_0 \int_V \sqrt{\tfrac{1}{2}\, \dot{\varepsilon}_{ij}\, \dot{\varepsilon}_{ij}}\, dV + \int_S \tau \cdot \Delta v \cdot \Delta s - \int_S T_i\, v_i\, ds \qquad (6)$$

This is Eq. (10) of Ref. 2.

The first term expresses the power for internal deformation over the volume of the deforming body ($\dot{W}_i$). The second term includes shear power over surfaces of velocity discontinuities, including the boundary between the die and billet. The last term covers the power supplied by pre-determined body traction such as back stress applied during wire drawing. J*, the externally supplied power, is provided by the front pull in wire drawing or by back stress in extrusion.

The power analysis is then performed by postulating a kinematically admissible velocity field and using it to calculate the internal power of deformation ($\dot{W}_i$), shear power ($\dot{W}_s$), friction power ($\dot{W}_f$), and any power due to application of external forces ($\dot{W}_b$). The upper bound on power may thus be written

$$J^* = \dot{W}_i + \dot{W}_s + \dot{W}_f + \dot{W}_b \qquad (6a)$$

Computation of powers involved:

(1) Internal power of deformation:

In zones I and III (Fig. 2) no deformations occur and therefore no internal power of deformation is involved. In zone II, using the spherical coordinate system, in the case of axial symmetry with respect to ϕ axis the strain rates are

$$\left.\begin{aligned}
\dot{\varepsilon}_{rr} &= \frac{\partial U_r}{\partial r} = 2\, V_f\, r_f^2\, \frac{\cos\theta}{r^3} \\
\dot{\varepsilon}_{\theta\theta} &= \frac{U_r}{r} = -V_f\, r_f^2\, \frac{\cos\theta}{r^3} \\
\dot{\varepsilon}_{\phi\phi} &= \frac{U_r}{r} = -V_f\, r_f^2\, \frac{\cos\theta}{r^3} \\
\dot{\varepsilon}_{r\theta} &= \frac{1}{2}\frac{1}{r}\frac{\partial U_r}{\partial \theta} = \frac{1}{2} V_f\, r_f^2\, \frac{\sin\theta}{r^3} \\
\dot{\varepsilon}_{\theta\phi} &= \dot{\varepsilon}_{\phi r} = 0
\end{aligned}\right\} \qquad (7)$$

This is Eq. 15 of Ref. 2.

For Mises' material, the internal power of deformation is

$$\dot{W}_i = \frac{2}{\sqrt{3}} \sigma_o \int_V \sqrt{\frac{1}{2} \dot{\varepsilon}_{ij} \dot{\varepsilon}_{ij}} \, dv \qquad (8)$$

(Eq. 16 of Ref. 2.)

Substituting the values for $\dot{\varepsilon}_{rr}$, $\dot{\varepsilon}_{\theta\theta}$, $\dot{\varepsilon}_{\phi\phi}$, and $\dot{\varepsilon}_{r\theta}$ into Eq. (8) and integrating,

$$\dot{W}_i = 2\pi \sigma_o R_f^2 v_f \, f(\alpha) \, \ln\left(\frac{R_o}{R_f}\right) \qquad (9)$$

(Eq. (20 of Ref. 2.)

For wire drawing, the power along the boundary on which the surface tractions are prescribed is that incident to the back tension $\dot{W}_b$;

$$\dot{W}_b = -\int_{St} T_i v_i \, ds = \pi V_o R_o^2 \sigma_{xb} = \pi V_f R_f^2 \sigma_{xb} \qquad (10)$$

(Eq. (13) of Ref. 2.)

Velocity discontinuities and friction losses:

Along surfaces Γ_1 and Γ_2 the power consumption is:

$$\dot{W}_{12} = \int_{S\Gamma_1\Gamma_2} T \cdot \Delta v \cdot ds$$

$$= \int_{S\Gamma_1} T \cdot \Delta v \cdot ds + \int_{S\Gamma_2} T \cdot \Delta v \cdot ds$$

Assuming the maximum shear stress of $\frac{\sigma_o}{\sqrt{3}}$ for Mises' material,

$$\dot{W}_{12} = \int_{\theta=0}^{\alpha} \sin^2\theta \, d\theta \; 4\pi r_f^2 v_f \frac{\sigma_o}{\sqrt{3}}$$

$$= \frac{2}{\sqrt{3}} \pi v_f R_f^2 \sigma_o \left[\frac{\alpha}{\sin^2\alpha} - \cot\alpha \right] \qquad (11)$$

(Eq. (21) of Ref. 2).

Along the conical portion of the boundary with the die, Γ_3, since hydrodynamic lubrication is assumed to prevail, there is a continuous film of lubricant between the die and billet. The shear loss over

the surface Γ_3 is given by

$$\dot{W}_{S_3} = \int_S \tau \cdot \Delta v \cdot ds \qquad (12)$$

where τ = shear stress in the lubricant film

Δv = difference in velocity of lubricant adhering to the die and deforming metal

ds = area of the conical surface

Hillier (30) calculated the shear power using the above formula. Using it together with Avitzur's (2) expression for internal power of deformation, he derived an expression for the relative drawing stress. He then compared his expression with the available experimental values. In calculating the shear power, he assumed, for simplicity, the fluid film thickness between the billet and die to be constant. His work is presented in Ref. 30.

In Ref. 35 Avitzur assumes that the thickness of the lubricant film varies from the entrance to the exit of the die and that the lubricant flow is always directed towards the apex of the cone, 0.

When hydrodynamic lubrication prevails, $\tau = \eta \frac{\Delta v}{h}$ (Eq. 4 of Ref. 30 and Eq. 5.26 of Ref. 35).

From geometry (Fig. 14),

$$ds = 2\pi R \frac{dR}{\sin\alpha}$$

$$\Delta v = v - 0 = v_f \left(\frac{R_f}{R}\right)^2 \cos\alpha$$

$$h = \frac{R}{R_f} \frac{\varepsilon}{\cos\alpha}$$

(Eq. 5.23 of Ref. 35)

Substituting the values into Eq. 12,

$$\dot{W}_{S_3} = \int_{R_f}^{R_o} \eta \frac{\left[v_f \left(\frac{R_f}{R}\right)^2 \cos\alpha\right]^2}{\frac{R}{R_f} \cdot \frac{\varepsilon}{\cos\alpha}} 2\pi R \frac{dR}{\sin\alpha}$$

$$\dot{W}_{S_3} = 2\pi V_f R_f^5 \frac{\cot\alpha}{\varepsilon} \cos^2\alpha \int_{R_f}^{R_o} \eta \frac{dR}{R^4}$$

Assuming the viscosity of the lubricant to be constant,

$$\dot{W}_{S3} = 2\pi V_f^2 R_f^5 \frac{\cot\alpha}{\varepsilon} \cos^2\alpha \, \eta \left[-\frac{1}{3}\frac{1}{R^3} \right]_{R_f}^{R_o}$$

$$= \frac{2}{3} \pi V_f^2 R_f^2 \cot\alpha \cos^2\alpha \frac{\eta}{\varepsilon} \left[1 - \left(\frac{R_f}{R_o}\right)^3 \right] \qquad (13)$$

Shear loss over the cylindrical portion of the die is:

$$\dot{W}_{S4} = \int \tau \cdot \Delta v \cdot ds$$

$$= \int \eta \frac{\Delta v^2}{h} ds$$

$$= \eta \frac{V_f^2}{\varepsilon} 2\pi R_f L$$

$$= 2\pi V_f^2 R_f^2 \frac{L}{R_f} \frac{\eta}{\varepsilon} \qquad (14)$$

Applied power:

The applied power

$$J^* = \pi V_f R_f^2 \sigma_{xf} \qquad (15)$$

When the lubricant film thickness is ε at exit, the final radius of the wire is $(R_f - \varepsilon)$. Substituting this value of R_f in Eqs. (9), (10), (11), (13), (14) and (15), and equating the applied power to the upper bound on energies,

$$\frac{\sigma_{xf}}{\sigma_o} = \frac{\sigma_{xb}}{\sigma_o} + 2 f(\alpha) \ln \frac{R_o}{R_f - \varepsilon} + \frac{2}{\sqrt{3}} \left[\frac{\alpha}{\sin^2\alpha} - \cot\alpha \right]$$

$$+ 2 \frac{V_f \eta}{\varepsilon \sigma_o} \left\langle \frac{\cot\alpha \cos^2\alpha}{3} \left[1 - \left(\frac{R_f - \varepsilon}{R_o} \right)^3 \right] + \frac{L}{R_f - \varepsilon} \right\rangle$$

$$\frac{\sigma_{xf}}{\sigma_o} = \frac{\sigma_{xb}}{\sigma_o} + 2 f(\alpha) \ln\left(\frac{R_o}{R_f}\right) + \frac{2}{\sqrt{3}}\left[\frac{\alpha}{\sin^2\alpha} - \cot\alpha\right]$$

$$+ 2 f(\alpha) \ln\left(1 + \frac{\varepsilon}{R_f}\right) + 2 \frac{V_f \eta}{R_f \sigma_o}\left\langle \cot\alpha \cos^2\alpha \left(\frac{R_f}{R_o}\right)^3 + \frac{L}{R_f}\right\rangle$$

$$+ 2 \frac{V_f \eta}{R_f \sigma_o} \frac{1}{(\varepsilon/R_f)}\left\langle \frac{\cot\alpha \cos^2\alpha}{3}\left[1 - \left(\frac{R_f}{R_o}\right)^3\right] + \frac{L}{R_f}\right\rangle \qquad (16)$$

The lubricant film thickness ε in the above expression is divided by the exit radius of the die, R_f, so as to make the term dimensionless $\left(\frac{\varepsilon}{R_f}\right)$ and to express the lubricant film thickness as a ratio of the exit radius of the die.

If ε is too small, the friction losses in Eq. (16) become excessive. If ε is too large, the reduction in area gets larger and the internal power of deformation is excessive. The draw stress of Eq. (16) as a function of ε exhibits a minimum. The minimum can be found by differentiation, as suggested by Hillier (30):

$$\frac{\partial(\sigma_{xf}/\sigma_o)}{\partial(\varepsilon/R_f)} = 0$$

$$= 2 f(\alpha) - 2 \frac{V_f \eta}{R_f \sigma_o} \frac{1}{(\varepsilon/R_f)^2}\left\langle \frac{\cot\alpha \cos^2\alpha}{3}\left[1 - \left(\frac{R_f}{R_o}\right)^3\right] + \frac{L}{R_f}\right\rangle$$

$$\therefore \left(\frac{\varepsilon}{R_f}\right) = \sqrt{\frac{V_f \eta}{R_f \sigma_o} \frac{1}{f(\alpha)}\left\langle \frac{\cot\alpha \cos^2\alpha}{3}\left[1 - \left(\frac{R_f}{R_o}\right)^3\right] + \frac{L}{R_f}\right\rangle} \qquad (17)$$

Substitution of this value of $\frac{\varepsilon}{R_f}$ in Eq. (16) leads to

$$\frac{\sigma_{xf}}{\sigma_o} = \frac{\sigma_{xb}}{\sigma_o} + 2 f(\alpha) \ln \frac{R_o}{R_f} + \frac{2}{\sqrt{3}}\left[\frac{\alpha}{\sin^2\alpha} - \cot\alpha\right]$$

$$+ 2 \frac{V_f \eta}{R_f \sigma_o}\left\langle \cot\alpha \cos^2\alpha \left(\frac{R_f}{R_o}\right)^3 + \frac{L}{R_f}\right\rangle$$

$$+ 4 \sqrt{\frac{V_f \eta}{R_f \sigma_o} f(\alpha)\left\langle \frac{\cot\alpha \cos^2\alpha}{3}\left[1 - \left(\frac{R_f}{R_o}\right)^3\right] + \frac{L}{R_f}\right\rangle} \qquad (18)$$

Equation (18) (Eq. 8.41 in Ref. 35) gives the relative drawing stress required for wire drawing with hydrodynamic lubrication.

Since compressive liquid pressure is positive, the relative hydro-

static pressure required for hydrostatic extrusion is given by.

$$\frac{P_b}{\sigma_o} = \frac{P_a}{\sigma_o} + 2 f(\alpha) \ln \frac{R_o}{R_f} + \frac{2}{\sqrt{3}} \left[\frac{\alpha}{\sin^2\alpha} - \cot\alpha\right]$$

$$+ 2 \frac{V_f \eta}{R_f \sigma_o} \left\langle \cot\alpha \cos^2\alpha \left(\frac{R_f}{R_o}\right)^3 + \frac{L}{R_f} \right\rangle$$

$$+ 4 \sqrt{\frac{V_f \eta}{R_f \sigma_o} f(\alpha) \left\langle \frac{\cot\alpha \cos^2\alpha}{3} \left[1 - \left(\frac{R_f}{R_o}\right)^3\right] + \frac{L}{R_f} \right\rangle} \quad (19)$$

The dimensionless term $\frac{V_f \eta}{R_f \sigma_o}$ (modified Sommerfeld number) expresses the effect of the lubricant. When this term increases, the lubricant film thickness $\frac{\varepsilon}{R_f}$ increases and hydrodynamic lubrication is more likely to prevail. In other words, an increase in viscosity (η) and exit velocity (V_f) and a decrease in final radius of billet (R_f) and the flow stress (σ_o) of the material of the billet tends to increase the possibility of hydrodynamic lubrication.

Criterion for hydrodynamic lubrication during wire drawing:

Rearranging Eq. (17),

$$\left(\frac{\varepsilon}{R_f}\right)^2 = \frac{V_f \eta}{R_f \sigma_o} \frac{1}{f(\alpha)} \left\langle \frac{\cot\alpha \cos^2\alpha}{3} \left[1 - \left(\frac{R_f}{R_o}\right)^3\right] + \frac{L}{R_f} \right\rangle \quad (20)$$

$$\text{i.e., } \frac{V_f \eta}{R_f \sigma_o} = \left(\frac{\varepsilon}{R_f}\right)^2 f(\alpha) \frac{1}{\left\langle \frac{\cot\alpha \cos^2\alpha}{3} \left[1 - \left(\frac{R_f}{R_o}\right)^3\right] + \frac{L}{R_f} \right\rangle}$$

$$\text{i.e., } V_f = \frac{R_f \sigma_o}{\eta} \left[\left(\frac{\varepsilon}{R_f}\right)^2 f(\alpha) \frac{1}{\left\langle \frac{\cot\alpha \cos^2\alpha}{3} \left[1 - \left(\frac{R_f}{R_o}\right)^3\right] + \frac{L}{R_f} \right\rangle}\right. \quad (21)$$

Equation (21) gives the critical exit velocity required to maintain hydrodynamic lubrication in terms of the process variables and the relative lubricant film thickness $\frac{\varepsilon}{R_f}$.

Equation (21) is plotted in Figs. 12 and 13. They represent the effect of required relative lubricant film thickness and semi-cone angle of the die on the critical exit velocity of the die ($r = 25\%$, $\frac{L}{R_f} = 0.2$, $\sigma_o = 50{,}000$ psi, $R_f = 0.25$ in., $\eta = 6 \times 10^{-5}$ lb sec/in^2).

The region above the lines of Figs. 12 and 13 represent the region where hydrodynamic lubrication will prevail. Suppose it is necessary to maintain a relative lubricant film thickness $\frac{\varepsilon}{R_f}$ of 0.05 in a particular wire drawing process. The region above the line corresponding to $\frac{\varepsilon}{R_f} = 0.05$ in Fig. 13 represents the region where hydrodynamic lubrication will prevail. Any velocity in that region will maintain hydrodynamic lubrication with a relative lubricant film thickness of 0.05, or higher.

Therefore, when the lubricant film thickness to be maintained is known, the critical exit velocity of wire can be read from Figs. 12 and 13. The lubricant film thickness to be maintained is determined from the roughness of the wire and die surfaces.

Criterion for hydrodynamic lubrication during hydrostatic extrusion:

Avitzur (2) has derived an expression for the extrusion pressure assuming constant friction factor:

$$\frac{P_b}{\sigma_o} = \frac{P_a}{\sigma_o} + 2 f(\alpha) \ln\left(\frac{R_o}{R_f}\right) + \frac{2}{\sqrt{3}} \left\{ \frac{\alpha}{\sin^2\alpha} - \cot\alpha + m \cot\alpha \ln\left(\frac{R_o}{R_f}\right) + m \frac{L}{R_f} \right\} \quad (22)$$

Substituting the value for $\frac{\eta V_f}{R_f \sigma_o}$ from Eq. (17) into Eq. (19),

$$\frac{P_b}{\sigma_o} = \frac{P_a}{\sigma_o} + 2\, f(\alpha) \ln\left(\frac{R_o}{R_f}\right) + \frac{2}{\sqrt{3}}\left[\frac{\alpha}{\sin^2\alpha} - \cot\alpha\right] + \frac{2\left\langle \cot\alpha \cos^2\alpha \left(\frac{R_f}{R_o}\right)^3 + \frac{L}{R_f}\right\rangle \left(\frac{\varepsilon}{R_f}\right)^2 f(\alpha)}{\left\langle \frac{\cot\alpha \cos^2\alpha}{3}\left[1 - \left(\frac{R_f}{R_o}\right)^3\right] + \frac{L}{R_f}\right\rangle} + 4 f(\alpha)\left(\frac{\varepsilon}{R_f}\right) \quad (23)$$

Equation (23) represents the pressure required for hydrostatic extrusion to maintain hydrodynamic lubrication with a relative lubricant film thickness of $\frac{\varepsilon}{R_f}$.

It is seen that, for a constant value of $\frac{\varepsilon}{R_f}$, the pressure required to extrude increases as the cone angle of the die increases.

Also, for a constant value of die angle, the pressure required for extrusion increases for higher values of relative lubricant film thickness, $\frac{\varepsilon}{R_f}$.

Equations (22) and (23) are plotted on the same graph for various values of friction factor and $\frac{\varepsilon}{R_f}$ (Fig. 10). The points where the curves of Eqs. (22) and (23) meet are of interest. Let the value of the cone angle corresponding to the point where the curves meet be α_{CR}. With semi-cone angles above this value, the pressure required to maintain a hydrodynamic fluid film of thickness $\frac{\varepsilon}{R_f}$ is more than the pressure required for extrusion with a friction factor m. Therefore, above α_{CR}, hydrodynamic lubrication is not likely to prevail. Conversely, below α_{CR}, the pressure required to maintain a hydrodynamic fluid film of thickness $\frac{\varepsilon}{R_f}$ is less than that required for extrusion with a friction factor m. Therefore, hydrodynamic lubrication will prevail below the critical cone angle α_{CR}.

α_{CR} can be determined from Eqs. (22) and (23).

Eliminating $\frac{P_b}{\sigma_o}$ from Eqs. (22) and (23), one gets

$$\frac{2}{\sqrt{3}} m \left[\cot\alpha \ \ln \frac{R_o}{R_f} + \frac{L}{R_f} \right] = \frac{2\left\langle \cot\alpha \cos^2\alpha \left(\frac{R_f}{R_o}\right)^3 + \frac{L}{R_f} \right\rangle \left(\frac{\varepsilon}{R_f}\right)^2 f(\alpha)}{\left\langle \frac{\cot\alpha \cos^2\alpha}{3} \left[1 - \left(\frac{R_f}{R_o}\right)^3\right] + \frac{L}{R_f} \right\rangle + 4 f(\alpha) \left(\frac{\varepsilon}{R_f}\right)} \quad (24)$$

Assuming L = 0, Eq. (24) reduces to

$$\frac{2}{\sqrt{3}} m \left[\cot\alpha \ \ln\left(\frac{R_o}{R_f}\right) + \frac{L}{R_f} \right] = \frac{6\left(\frac{R_f}{R_o}\right)^3 \left(\frac{\varepsilon}{R_f}\right)^2 f(\alpha)}{\left[1 - \left(\frac{R_f}{R_o}\right)^3\right]} + 4 f(\alpha) \frac{\varepsilon}{R_f}$$

$$\frac{m}{\sqrt{3}} \left[\cot\alpha \ \ln\left(\frac{R_o}{R_f}\right) \right] = \frac{3\left(\frac{\varepsilon}{R_f}\right)^2 f(\alpha)}{\left[\left(\frac{R_o}{R_f}\right)^3 - 1\right]} + 2 f(\alpha) \left(\frac{\varepsilon}{R_f}\right)$$

$$\frac{m}{\sqrt{3}} \left[\cot\alpha \ \ln \frac{R_o}{R_f} \right] = \left\{ \frac{3\left(\frac{\varepsilon}{R_f}\right)^2 f(\alpha)}{\left[\left(\frac{R_o}{R_f}\right)^3 - 1\right]} + 2 f(\alpha) \left(\frac{\varepsilon}{R_f}\right) \right\}$$

$$\cot\alpha_{CR} = \frac{\sqrt{3}}{m \ln\left(\frac{R_o}{R_f}\right)} \left[\frac{3\left(\frac{\varepsilon}{R_f}\right)^2 f(\alpha)}{\left\{\left(\frac{R_o}{R_f}\right)^3 - 1\right\}} + 2 f(\alpha) \left(\frac{\varepsilon}{R_f}\right) \right]$$

$$\alpha_{CR} = \cot^{-1} \left\{ \frac{\sqrt{3}}{m \ln\left(\frac{R_o}{R_f}\right)} \left[\frac{3\left(\varepsilon/R_f\right)^2 f(\alpha)}{\left[\left(\frac{R_o}{R_f}\right)^3 - 1\right]} + 2 f(\alpha) \left(\frac{\varepsilon}{R_f}\right) \right] \right\} \quad (25)$$

Figure 11 plotted from Eq. (25) represents the effect of friction factor and lubricant film thickness on the critical semi-cone angle of the die.

If the friction factor and the minimum lubricant film thickness to be maintained are known for the process, the critical cone angle below which hydrodynamic lubrication will prevail can be predicted from Fig. 11 or Eq. (25). The friction factor is determined from the material of the die and billet.

EXPERIMENTAL PROCEDURE

The object of the experiment was to determine whether hydrodynamic lubrication prevails during hydrostatic extrusion and if it prevails, under what combination of the process variables. It was decided to hydrostatically extrude through dies of various cone angles for the same reduction of area and exit diameter. It was also decided that the surface of the billet would be marked in some way so that the marking could be studied after extrusion. If the marking was not affected after extrusion, it was likely that hydrodynamic lubrication was prevailing, and vice-versa.

Sample preparation:

Drill rod (1% carbon steel) $\frac{5}{16}$ in. in diameter was used as the billet. A length of 3 in. was chosen so as to prevent sudden full extrusion. It was feared that if full extrusion occurred at high extrusion velocities, the surface of the billet would be marred by striking the bottom of the extrusion chamber. The ends of the billet were made square.

It was known that electroplated silver is a uniform coating that adheres strongly to the billet surface. It was also known that silver plating adheres better if the billet surface is first plated with gold.

Atomex gold plating solution was heated until fumes evolved. The thoroughly cleaned billet was immersed in this solution for a few seconds to thinly plate it with gold. The billet was then removed and dried.

In the silver plating process, solid silver was used as the anode while the gold plated billet was used as the cathode. Both were immersed without touching in an electrolyte solution made of 500 ml of water, 12.30 gm of silver cyanide, 15.00 gm of potassium cyanide, and 11.23 gm of potassium carbonate. The anode and cathode were connected to the D.C. power supply through a rheostat, an ammeter and a switch. A current of 0.025 amps was applied for about 45 minutes. A uniform layer of silver was plated over the surface of the billet and the billet was ready for extrusion.

Details of Experiment:

Dies with identical exit diameters of 0.25 in. and 5°, 10°, 15°, 22.5°, 30°, and 40° semi-cone angles were used.

The extrusion was conducted in the equipment shown in Fig. 15 using SAE 10 motor oil as the pressurizing fluid with no receiver pressure.

Pressure is developed in the pressurizing fluid by means of a hand pump. When the required pressure is reached the billet starts extruding. As the billet shoots through the die, the pressure at the entrance side of the die decreases and the extrusion stops when the pressure is not sufficient to extrude the billet (the process is very fast and it is impossible to maintain the pressure to get complete extrusion by handpumping). The position where extrusion stopped is marked in Figs. 17 and 19. If another extrusion of the same billet is required, it can be accomplished by raising the pressure again by handpumping. If desired, the billet can be fully extruded by repeating the process.

Experimental Results:

The extruded billets are shown in Figs. 16-21. It can be seen from Figs. 16-19 (semi-cone angles of 5°, 10°, 15°, and 22.5°) that the silver coating at the front end of the billets are scraped off while at the rear end it is unaffected. This implies that after initial metal-to-metal contact between the die and billet, the extrusion took place with hydrodynamic lubrication. Figures 20 and 21 (semi-cone angles 30° and 40°) show extrusions without hydrodynamic lubrication so that the silver coating on the billet surfaces were scraped off end to end.

It is evident from Figs. 16-21 that hydrodynamic lubrication prevails with lower values of die semi-cone angle only (when the values of the other process variables remain constant). This is because, for smaller values of die semi-cone angles, the pressure required for hydrostatic extrusion with hydrodynamic lubrication is less as compared to one without hydrodynamic lubrication, and vice versa (see Fig. 10).

DISCUSSION AND CONCLUSIONS

Expressions were derived using the upper bound approach for the evaluation of the force required in wire drawing and the pressure required in hydrostatic extrusion, assuming a continuous lubricant film thickness between the die and billet. Criteria for the existence of hydrodynamic lubrication during wire drawing and hydrostatic extrusion were derived from these expressions and Eq. 30 of Ref. 2.

The effects of each of the process variables on the pressure and lubricant film thickness are presented in Figs. 22-31. Conclusions are drawn with the assumption of constant friction factor.

The effect of semi-cone angle and die land on the expected relative lubricant film thickness is shown in Fig. 22a. It is seen that for a constant die land length, the expected relative lubricant film thickness decreases as the semi-cone angle of the die increases. This indicates that, to maintain a thick lubricant film, a die with a relatively small cone angle should be used. Also, as the length of the die land is increased, the expected lubricant film thickness also increases. So, to establish hydrodynamic lubrication, a die with relatively small cone angle and relatively long land should be used. In Figs. 22a and 22b, if the required lubricant thickness $\left(\frac{\varepsilon}{R_f}\right)_{CR}$ is below the expected thickness (below the respective line) then hydrodynamic lubrication prevails. It should be remembered that lengthening the die land increases the friction.

The effect of die land length and die semi-cone angle on the critical relative lubricant film thickness is shown in Fig. 22b. For

a constant die land the critical relative lubricant film thickness at first decreases and then remains constant as the die semi-cone angle is increased.

The effects of die land length, critical relative lubricant film thickness, percent reduction, and die semi-cone angle on the modified Sommerfeld number during wire drawing are presented in Figs. 22c-22e.

The effect of die land length and die semi-cone angle on the modified Sommerfeld number in hydrostatic extrusion is shown in Fig. 23. For a constant die land length, the modified Sommerfeld number increases at first and then decreases as the die semi-cone angle is increased.

The effect of die semi-cone angle on the critical relative lubricant film thickness is shown in Fig. 24. As the die semi-cone angle increases, the lubricant film thickness decreases. This again implies that hydrodynamic lubrication will prevail with smaller cone angles.

The effect of receiver pressure and die semi-cone angle on the extrusion pressure is shown in Fig. 25. As the receiver pressure is increased, the pressure required for extrusion also increases by that amount. For a constant value of receiver pressure, as the semi-cone angle of the die is increased, the extrusion pressure decreases at first and then increases. The lowest extrusion pressure corresponds to the optimum semi-cone angle.

The relative extrusion pressure decreases at first and then increases as the semi-cone angle of the die increases for a constant value of modified Sommerfeld number. This is shown in Fig. 26.

Figure 27 shows that the critical lubricant film thickness decreases as the semi-cone angle of the die increases for a constant value of

modified Sommerfeld number. This again implies that hydrodynamic lubrication prevails with smaller cone angles. As the modified Sommerfeld number increases, the critical lubricant film thickness increases for a constant die semi-cone angle.

The effect of percent reduction and die semi-cone angle on the critical relative lubricant film thickness is shown in Fig. 28. For a constant reduction of area, the critical relative lubricant film thickness decreases with increasing die semi-cone angle. As the percent reduction gets larger, the lubricant film thickness increases for a constant die semi-cone angle. Hydrodynamic lubrication can be expected with higher reduction and smaller die semi-cone angle while the values of the other process variables remain constant.

The effect of percent reduction and die semi-cone angle on the extrusion pressure is shown in Fig. 29. As the reduction gets larger, the extrusion pressure also increases for a constant semi-cone angle. The extrusion pressure at first decreases and then increases, as the semi-cone angle of the die is increased for a constant reduction of area. The lowest pressure corresponds to the optimum cone angle for that particular percent reduction of area.

The effect of extrusion pressure and die semi-cone angle on the expected relative lubricant film thickness and modified Sommerfeld number is shown in Figs. 30 and 31. As the semi-cone angle of the die is increased, the modified Sommerfeld number increases at first and then decreases for a constant value of extrusion pressure. The modified Sommerfeld number increases as the extrusion pressure is increased for a constant value of die semi-cone angle. As the extrusion pressure is

increased, the expected lubricant film thickness increases for a constant value of die cone angle. It decreases as the die semi-cone angle is increased.

The following observations can be made for both wire drawing and hydrostatic extrusion:

(1) The velocity of the deforming material over the conical surface of the die must reach a critical value in order to produce a complete separation of die and billet. When this velocity is reached or exceeded, hydrodynamic lubrication prevails.

(2) The die semi-cone angle plays an important role in maintaining hydrodynamic lubrication. The smaller the semi-cone angle, the higher the velocity at the conical surface of the die (for a particular combination of reduction and die land length) and hence the greater the tendency for hydrodynamic lubrication to prevail.

(3) An increase in die land length tends to increase the lubricant film thickness for a constant value of the other process variables (see Eq. 22).

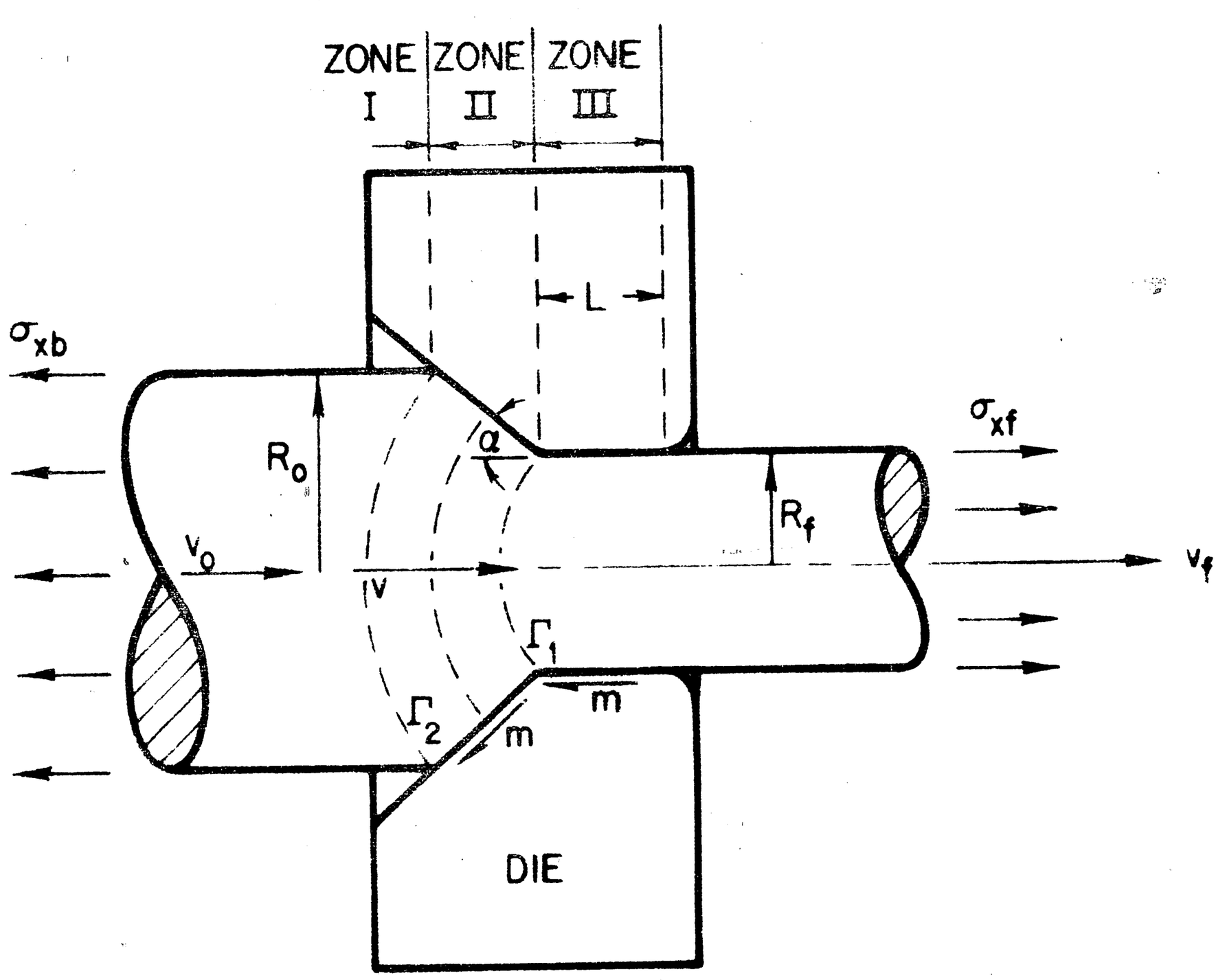

FIG. 1 THE DIE AND WIRE IN WIRE DRAWING AND EXTRUSION.

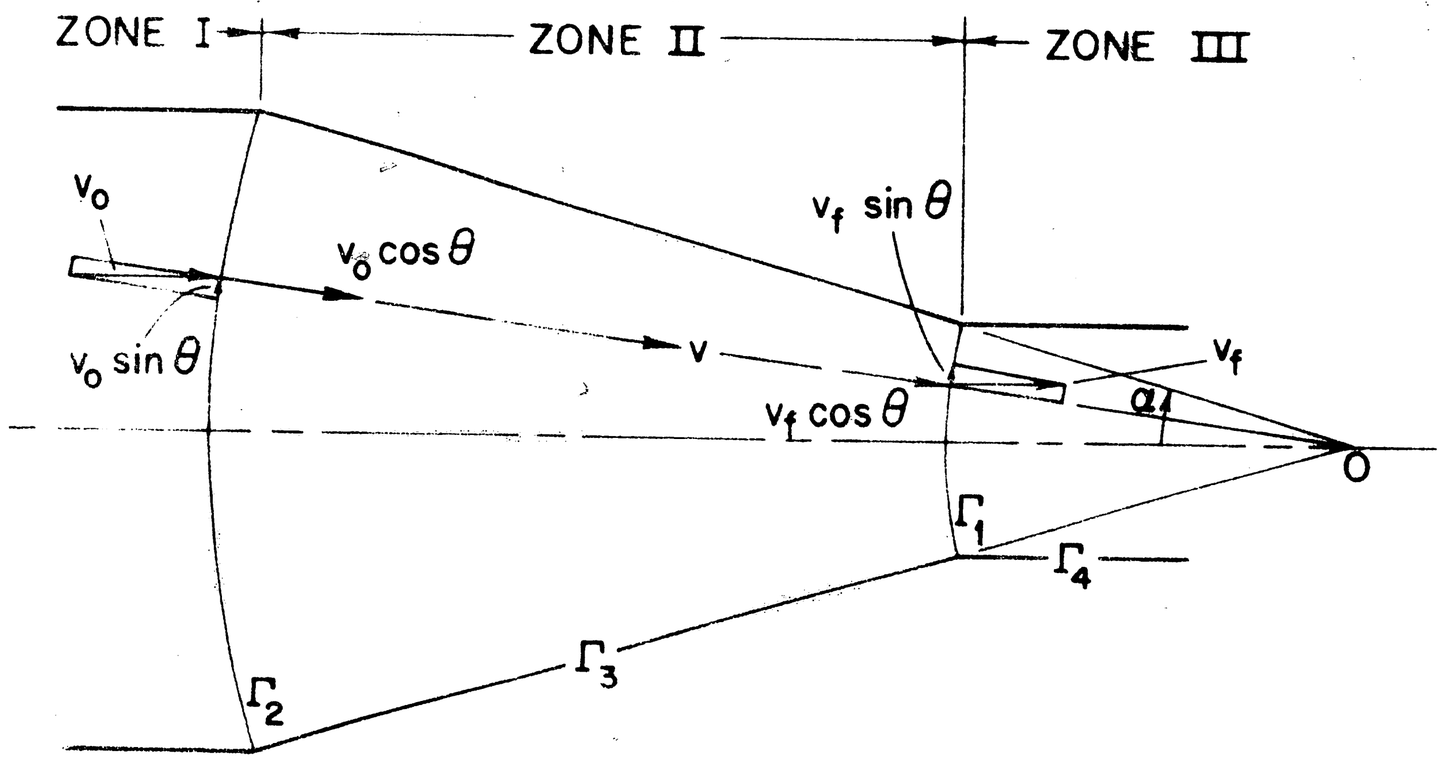

FIG. 2 KINEMATICALLY ADMISSIBLE VELOCITY FIELD.
(FIG. 2 OF REF 2)

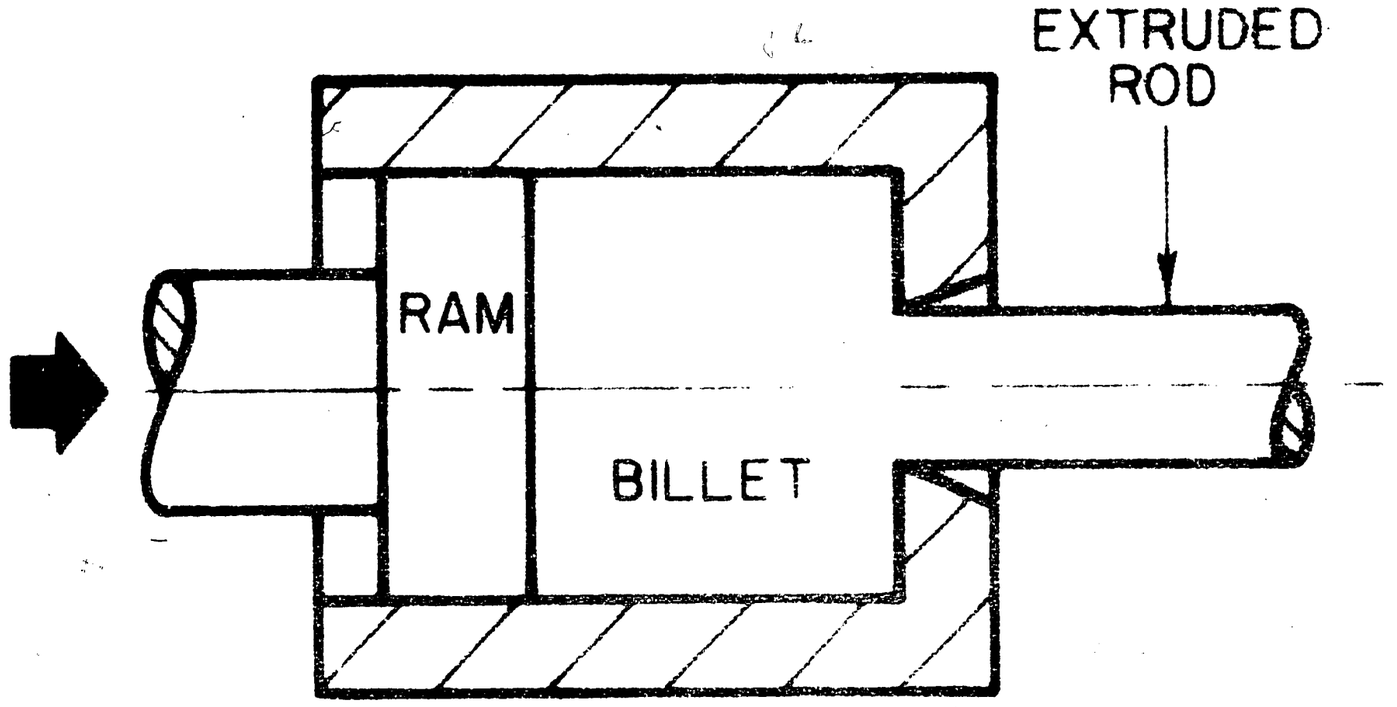

(a)

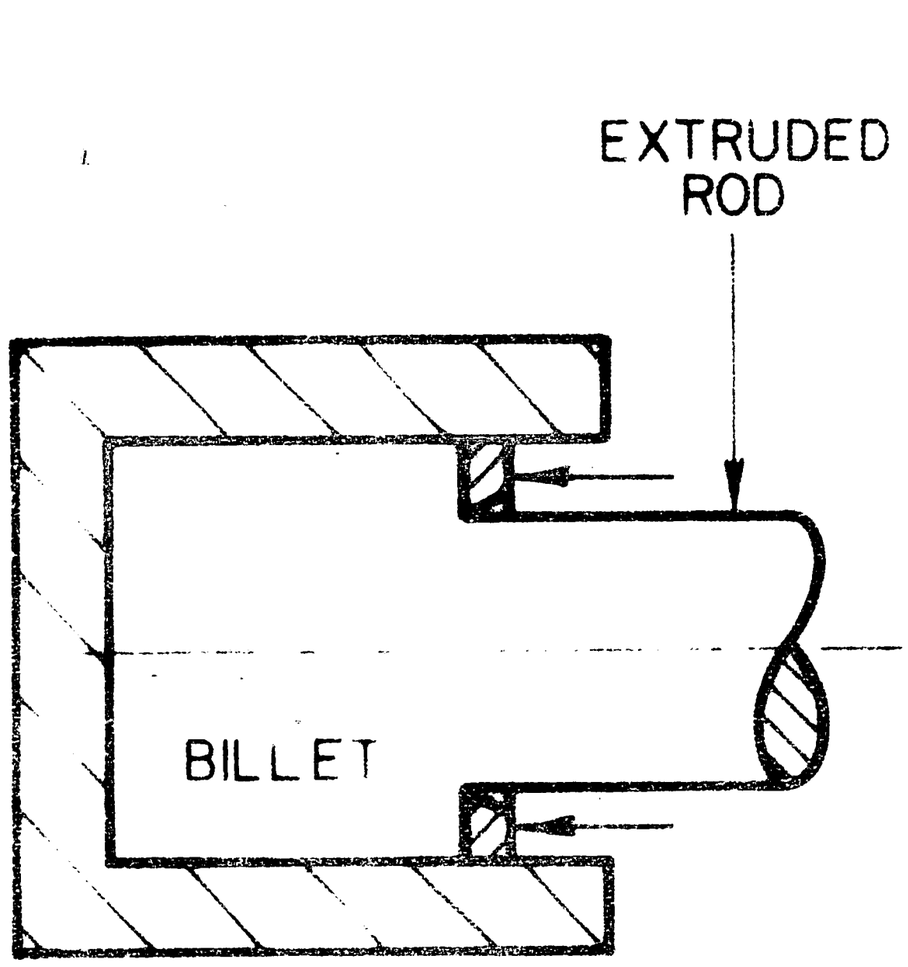

(b)

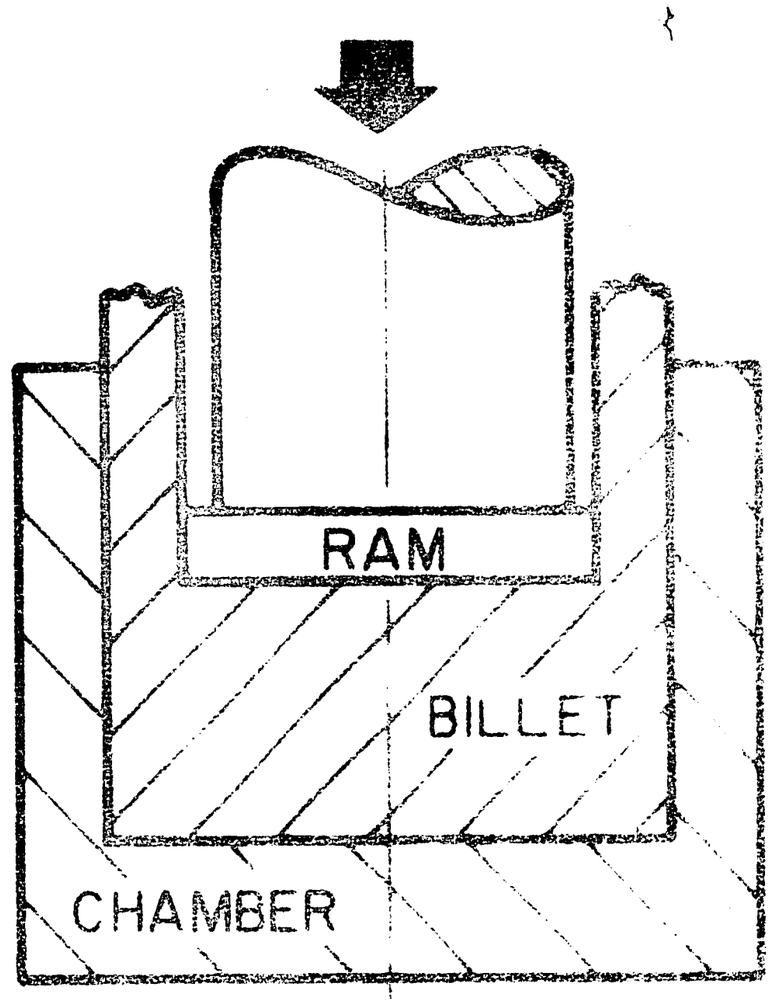

(c)

FIG. 3 DIRECT(a), INDIRECT(b), AND IMPACT EXTRUSION (c)

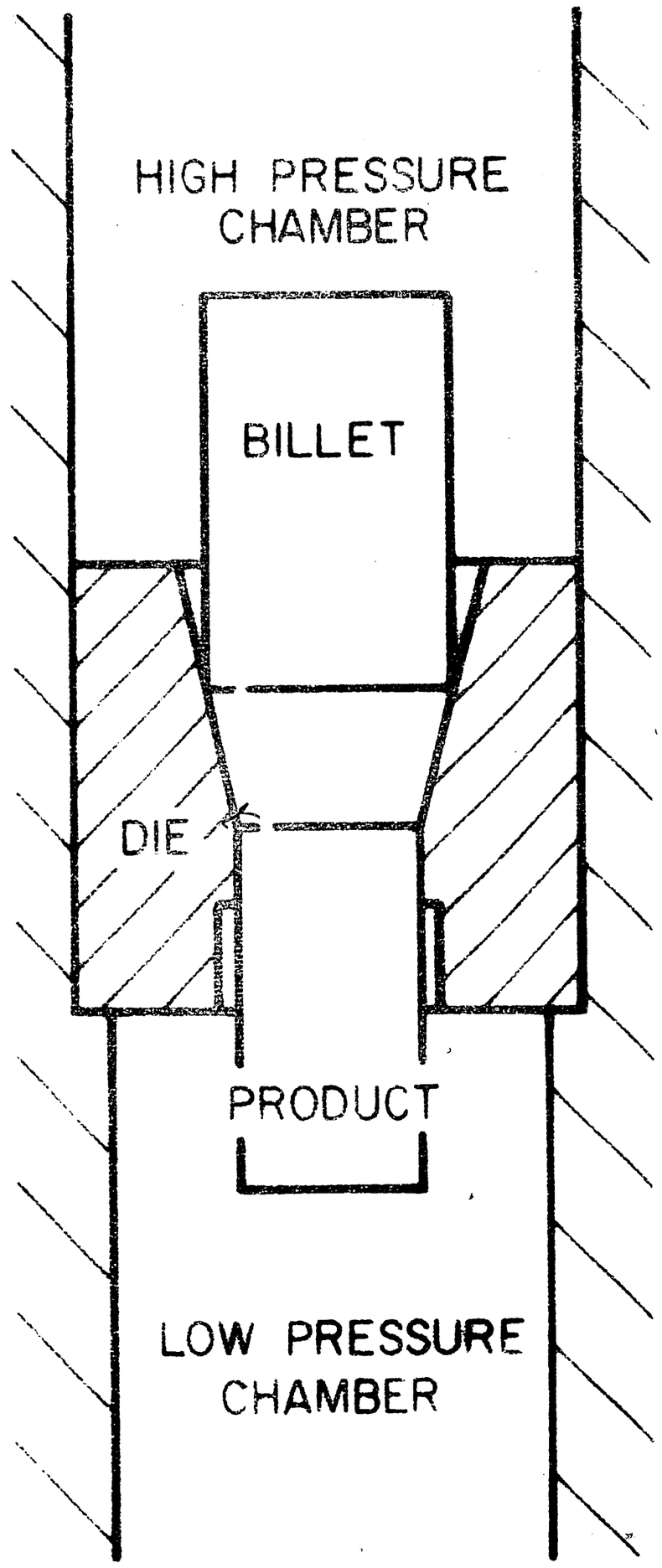

FIG. 4 HYDROSTATIC EXTRUSION.

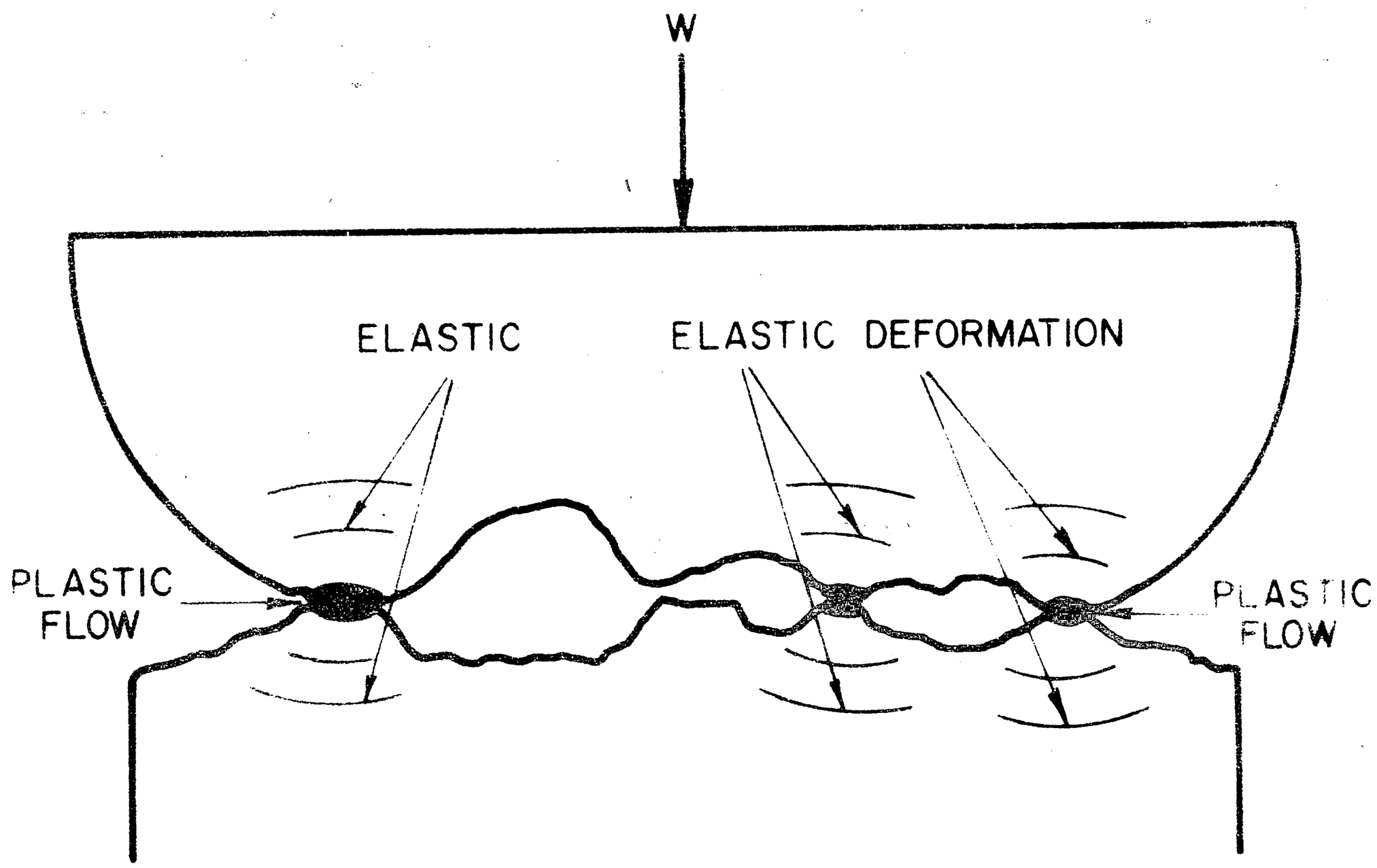

FIG. 5 SCHEMATIC OF SURFACE CONTACT

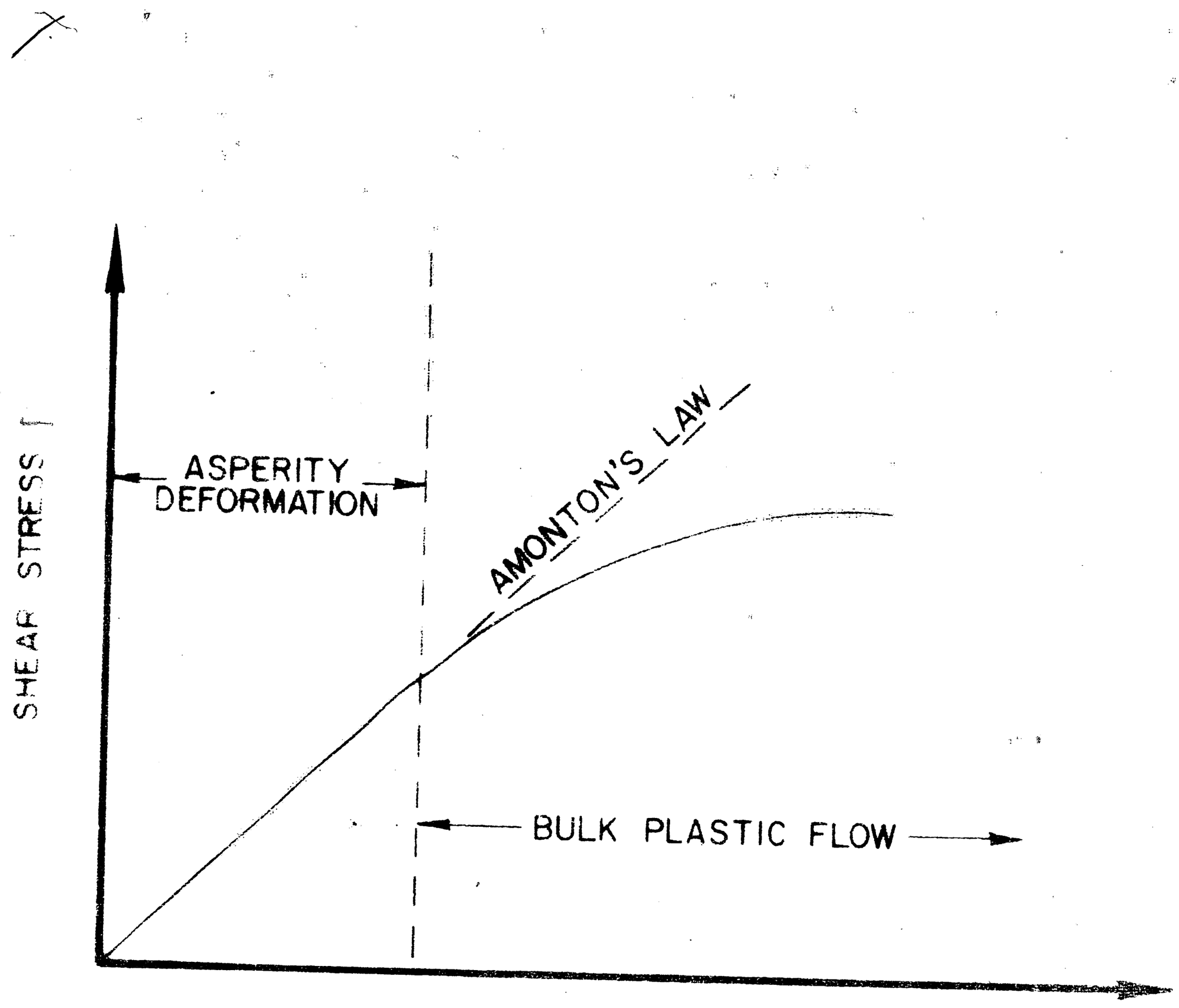

FIG. 6 VARIATION OF SLIDING – CONTACT SHEAR STRESS WITH CONTACT STRESS SHOWING DEVIATION FROM AMONTON'S LAW. FIG. 12 (PAGE 73) OF REF. 22

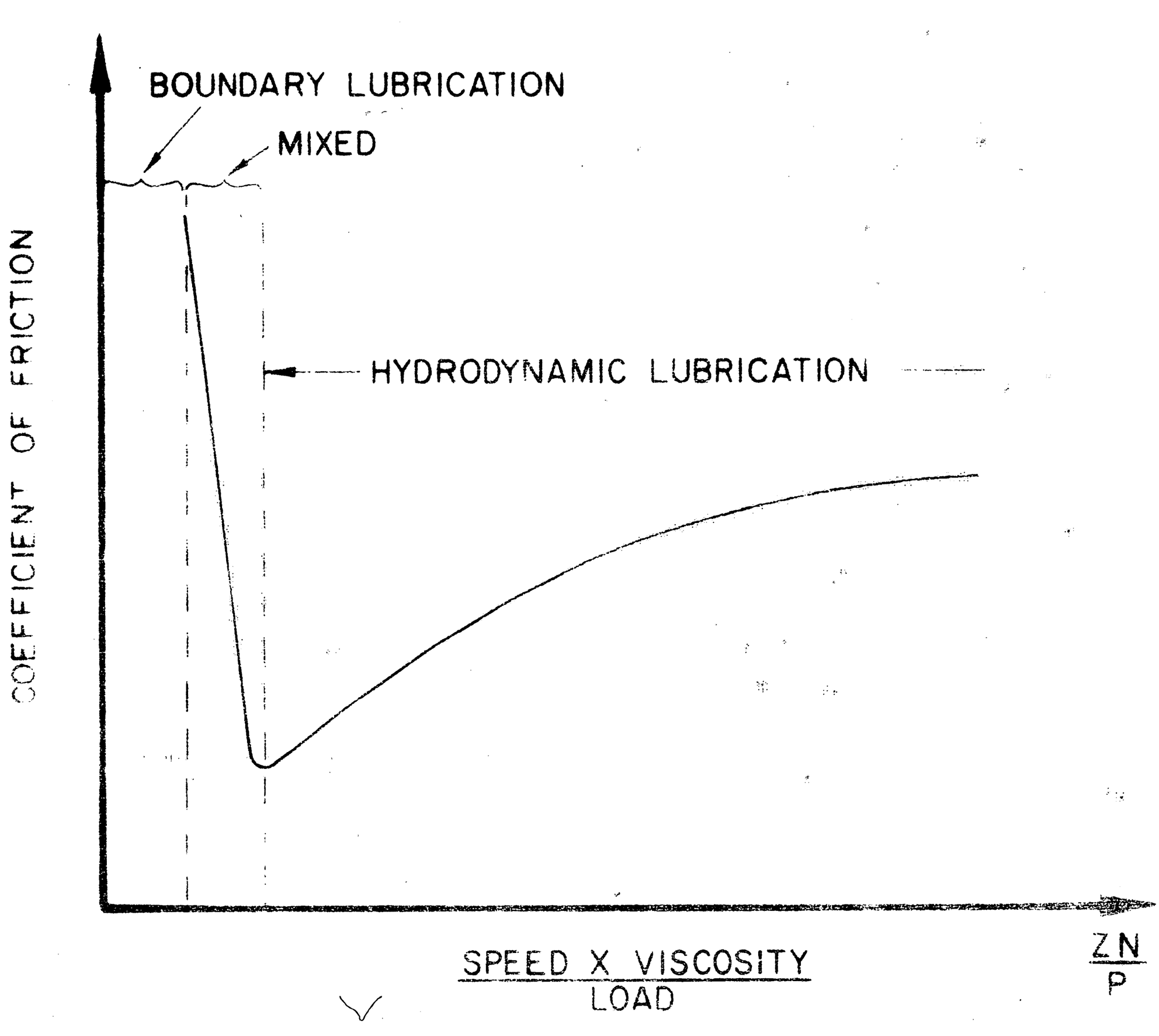

FIG.7 STRIBECK CURVE. (STRIBECK'S REF. 25)

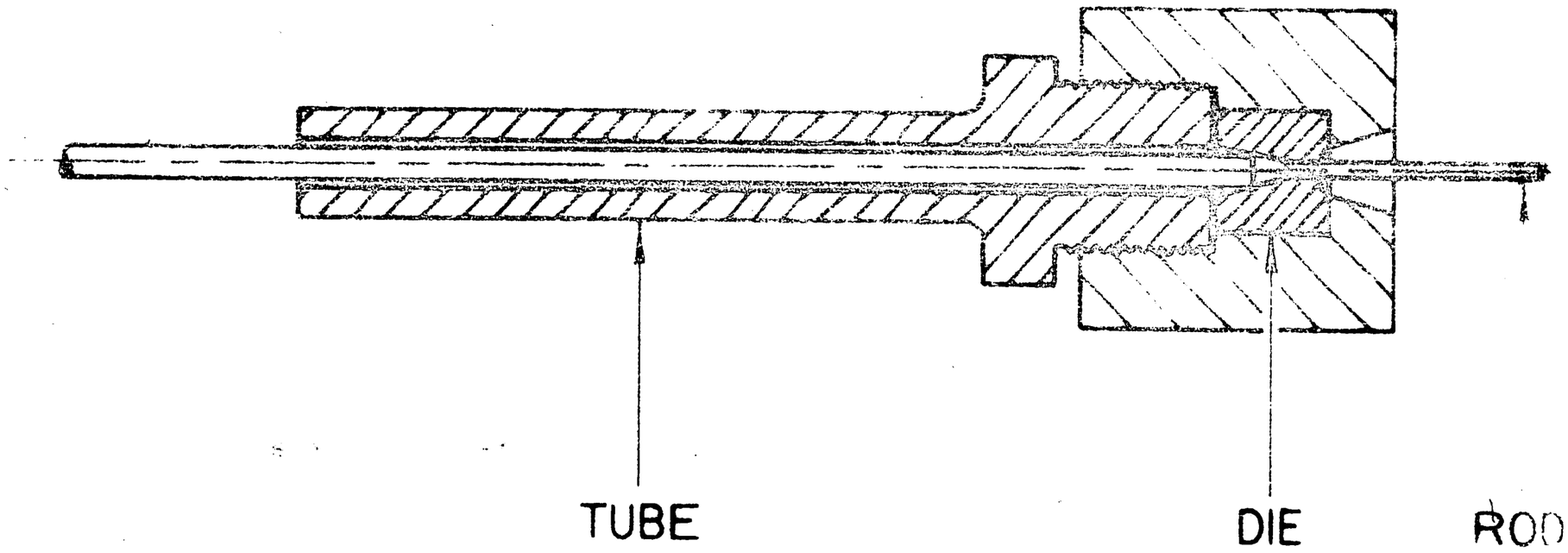

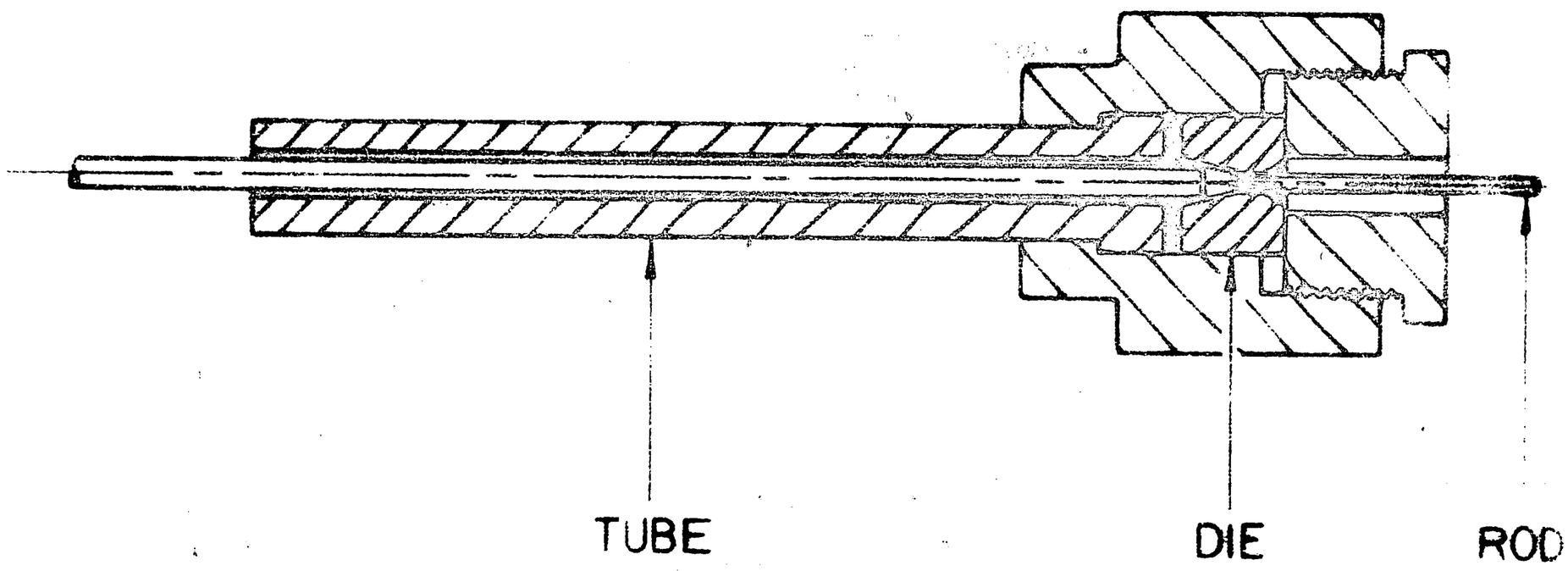

FIG. 8 TYPICAL ARRANGEMENT OF INLET TUBE AND DIE.
(FIG. 1 OF CHRISTOPHERSON'S REF. 31)

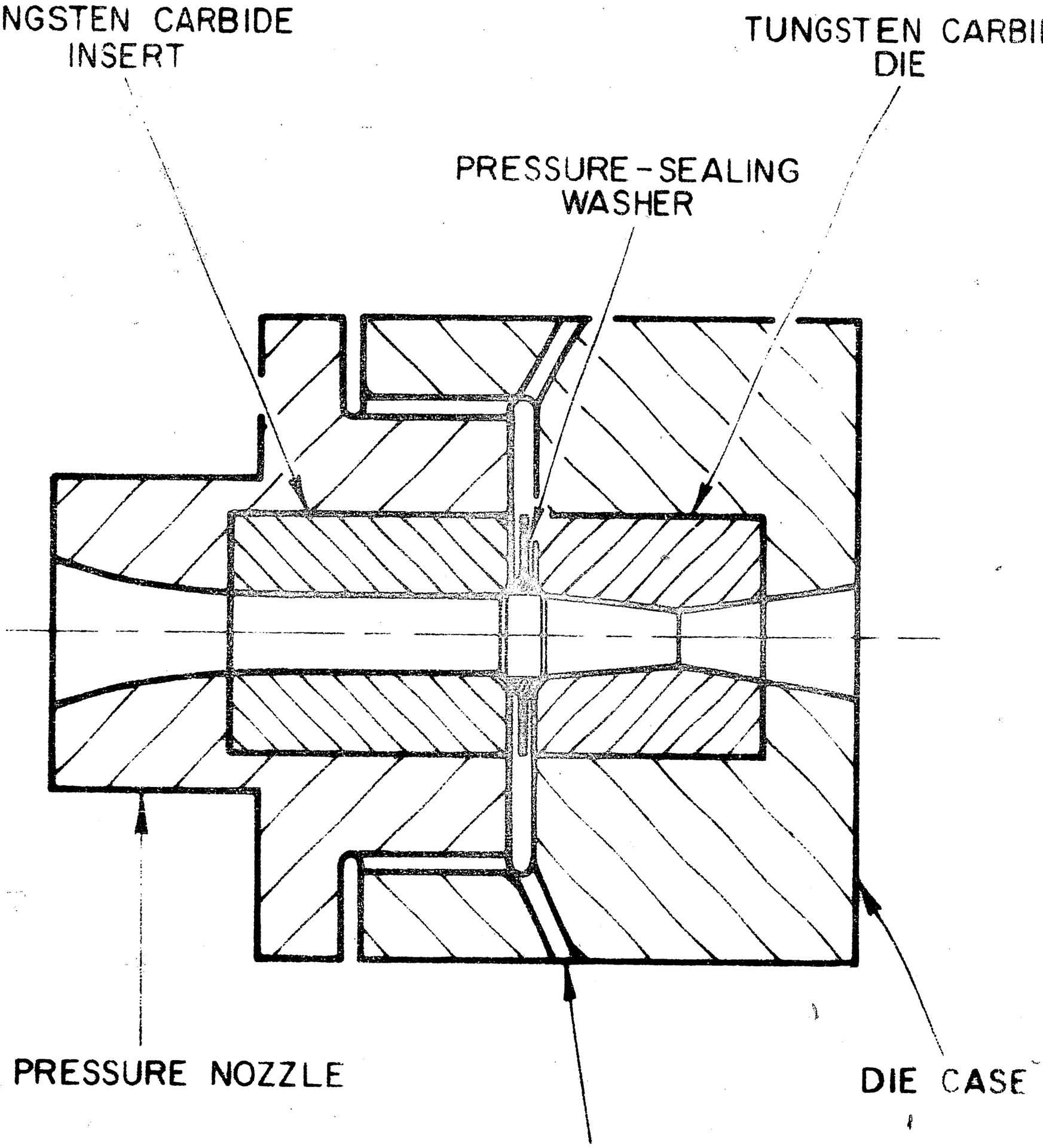

FIG. 9 CROSS SECTION OF BISRA NOZZLE DIE UNIT FOR HYDRODYNAMIC LUBRICATION DRAWING WITH DRY SOAP. (FIG. 20 OF BISRA'S REF. 22 PAGE 97)

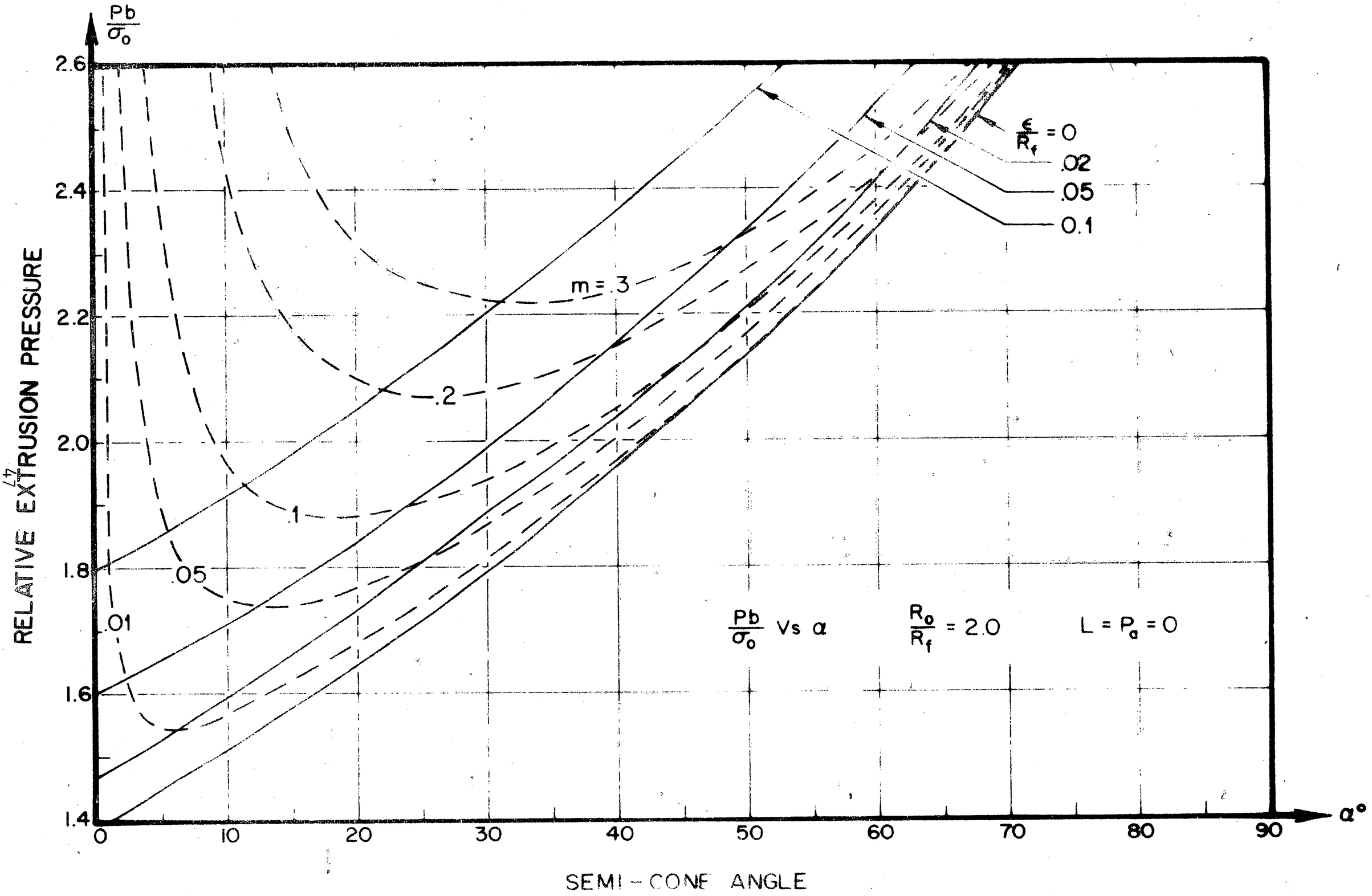

FIG. 10 EFFECT OF RELATIVE LUBRICANT FILM THICKNESS AND DIE SEMI-CONE ANGLE ON RELATIVE EXTRUSION PRESSURE DURING HYDROSTATIC EXTRUSION.

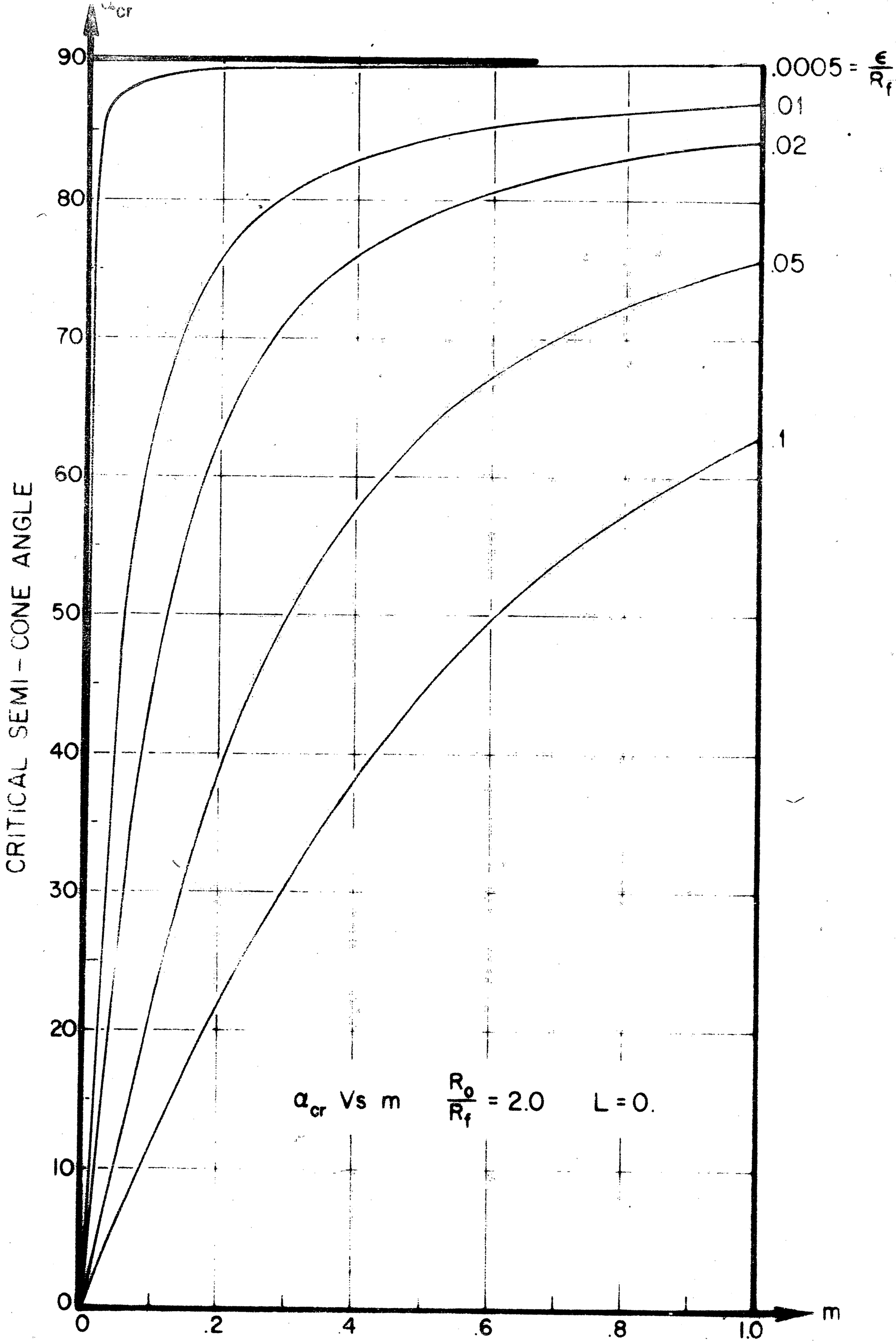

FIG. 11 EFFECT OF RELATIVE LUBRICANT FILM THICKNESS AND FRICTION FACTOR ON CRITICAL DIE SEMI-CONE ANGLE DURING HYDROSTATIC EXTRUSION.

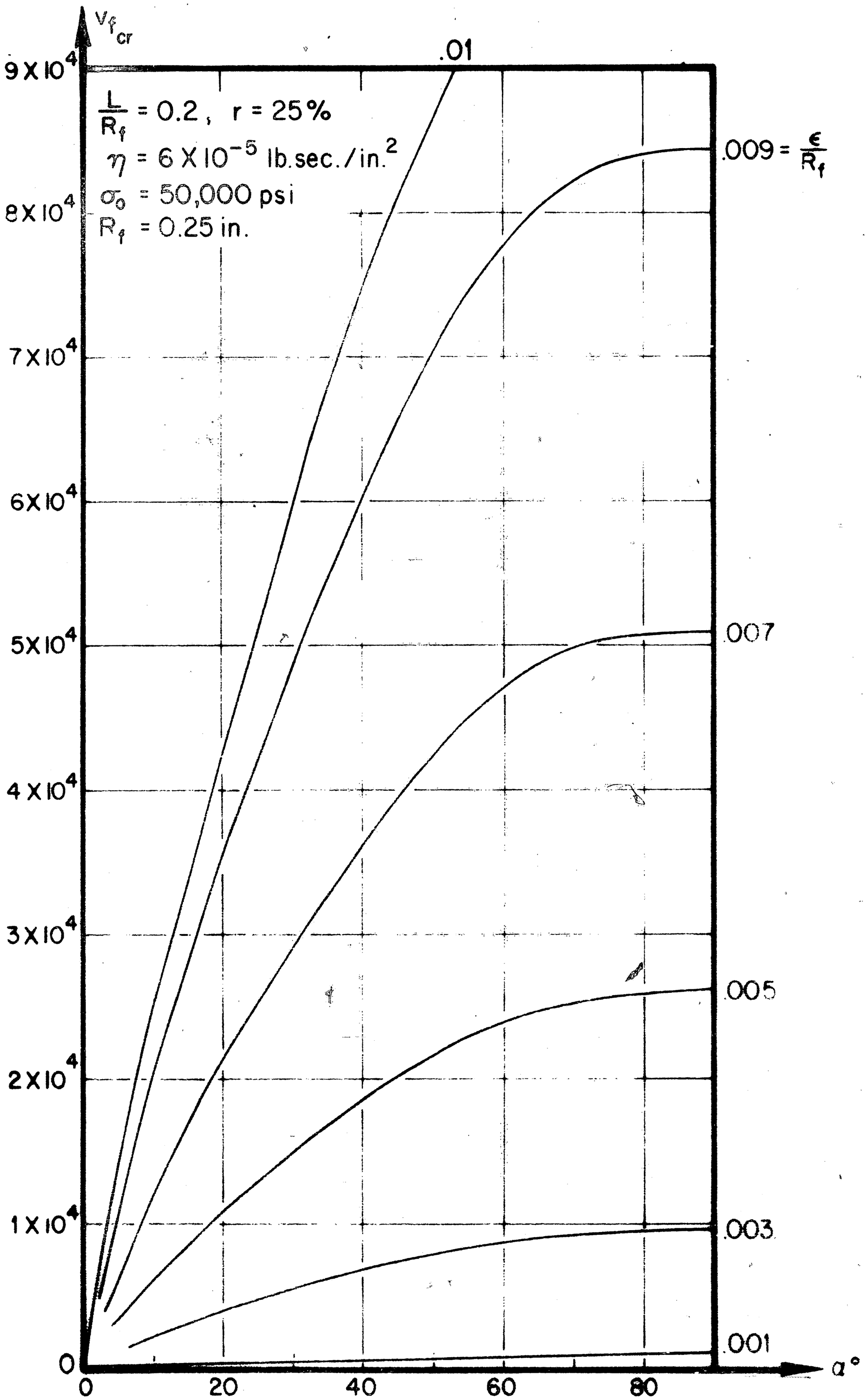

FIG. 12 EFFECT OF RELATIVE LUBRICANT FILM THICKNESS AND DIE SEMI-CONE ANGLE ON CRITICAL EXIT VELOCITY OF WIRE DURING WIRE DRAWING.

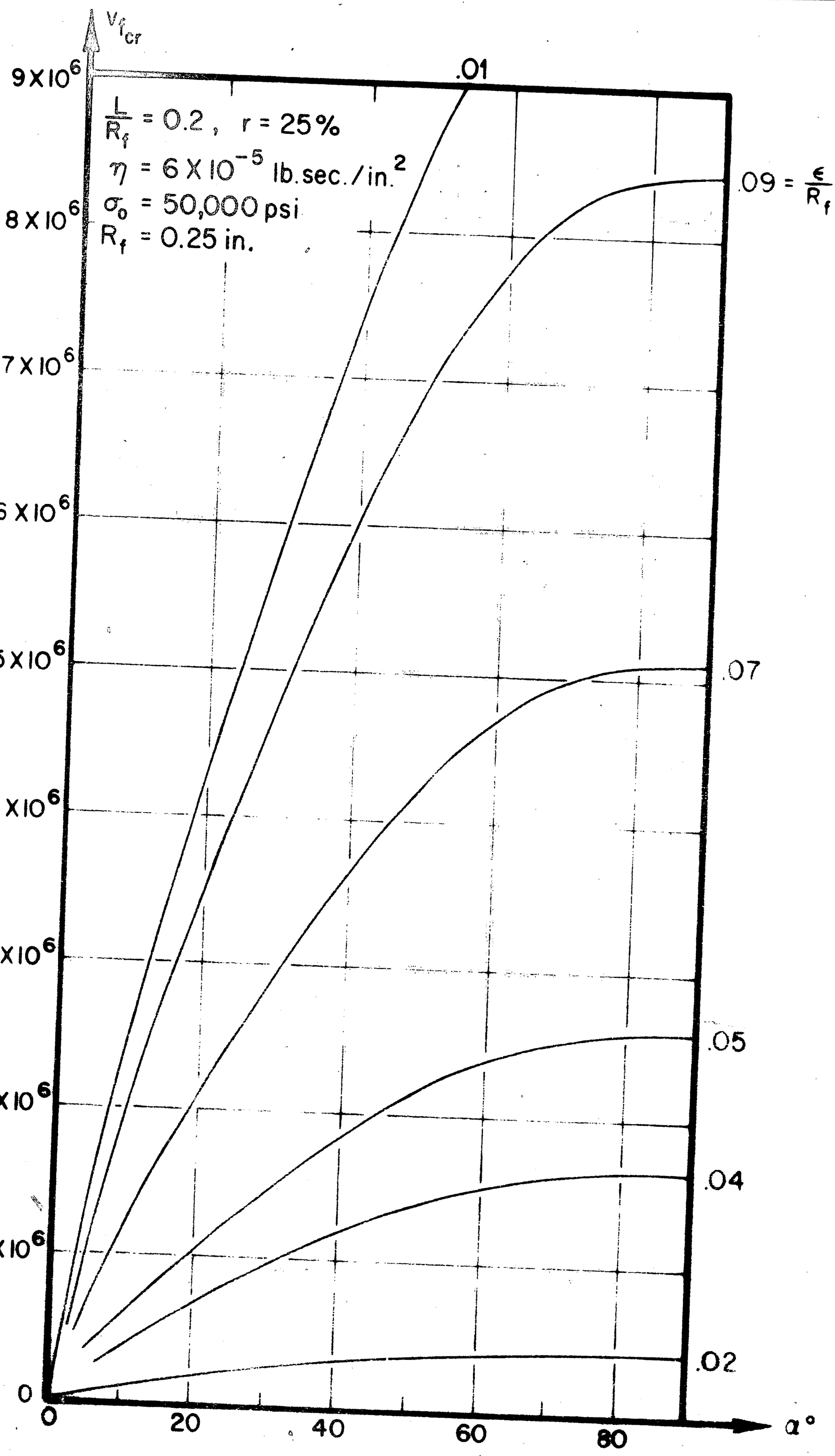

FIG. 13 EFFECT OF RELATIVE LUBRICANT FILM THICKNESS AND DIE SEMI-CONE ANGLE ON CRITICAL EXIT VELOCITY OF WIRE DURING WIRE DRAWING.

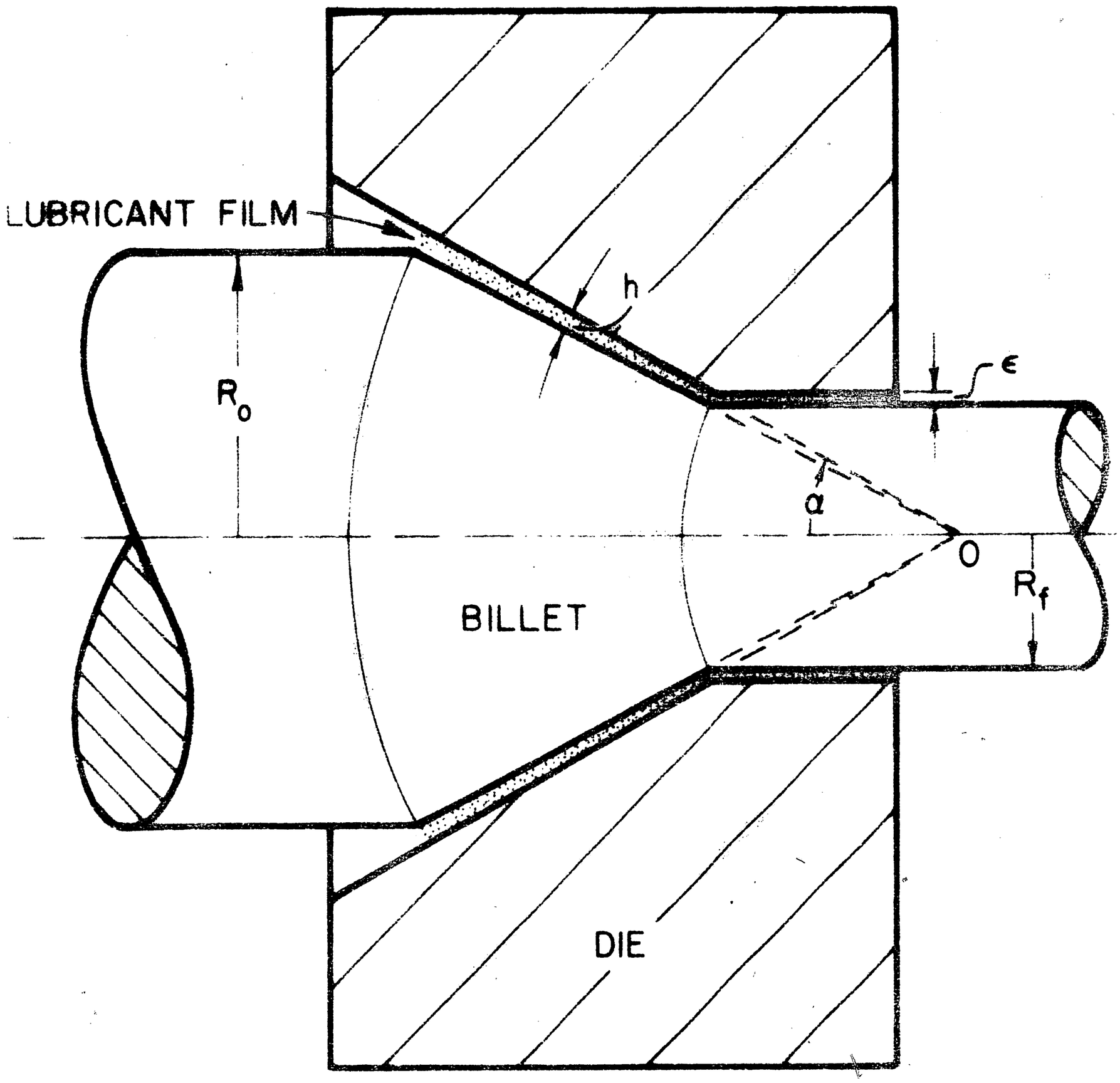

FIG. 14 DIE, BILLET, AND LUBRICANT FILM WHEN HYDRO – DYNAMIC LUBRICATION PREVAILS BETWEEN DIE AND BILLET.

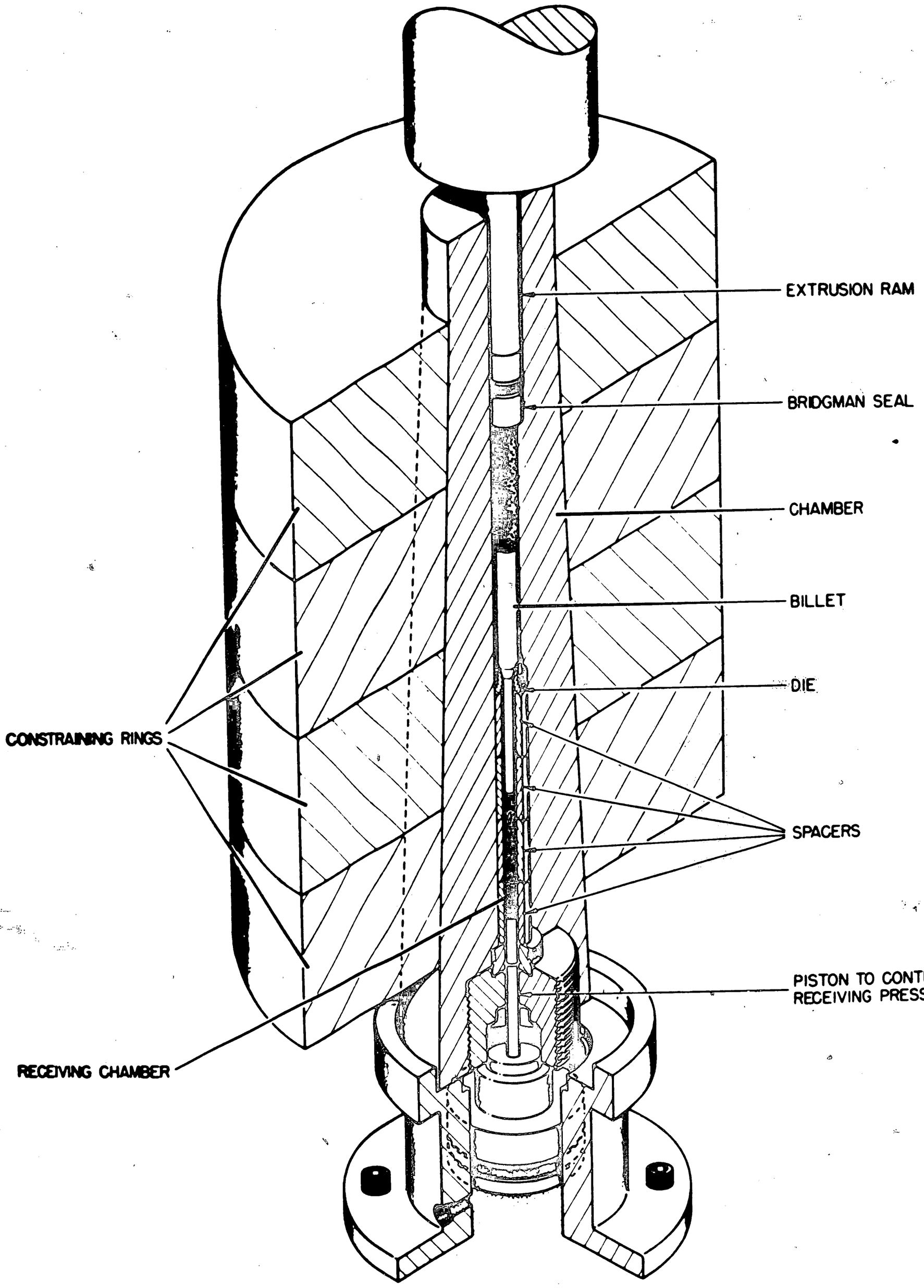

Fig. 15 Hydrostatic extrusion equipment (Lehigh University chamber by Pressure Technology Corporation of America)

α = 5° Reduction = 36% Max. Pressure = 135,000 psi Min. Pressure = ? (Die Broken)

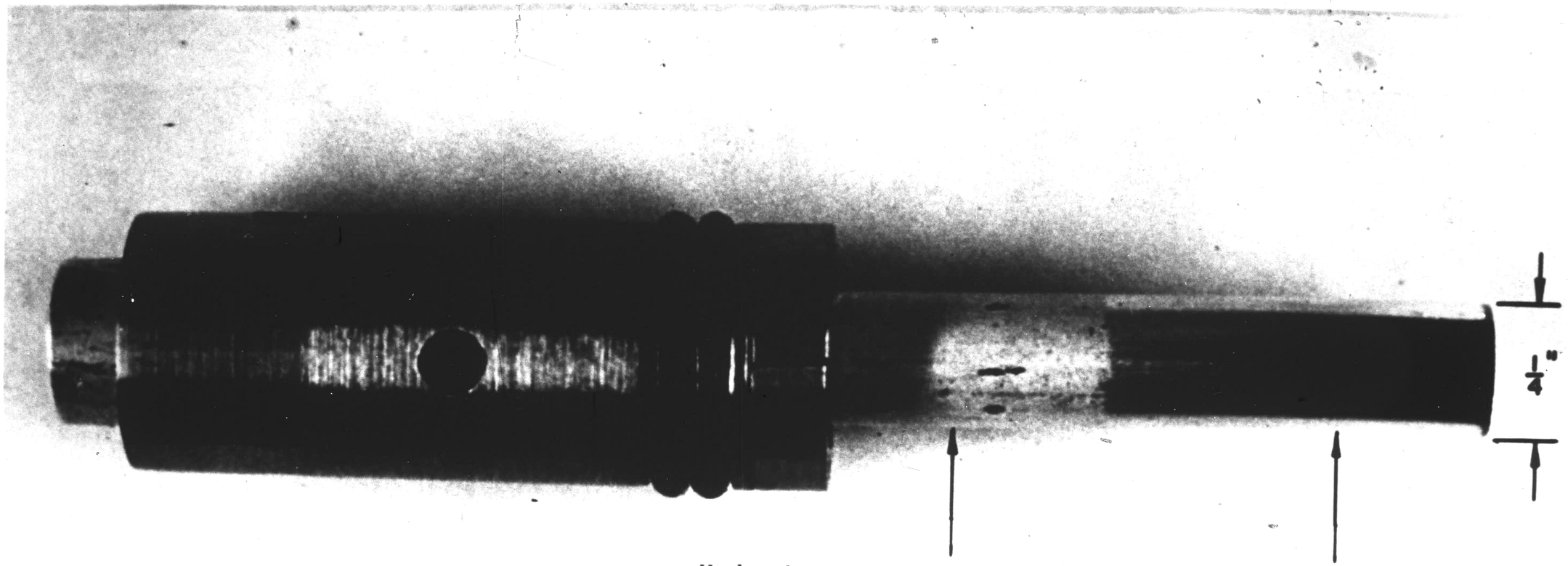

Fig. 16 Die and billet after hydrostatic extrusion

α = 10° Reduction = 36% Max. Pressure = 100,000 psi Min. Pressure = 64,000 psi

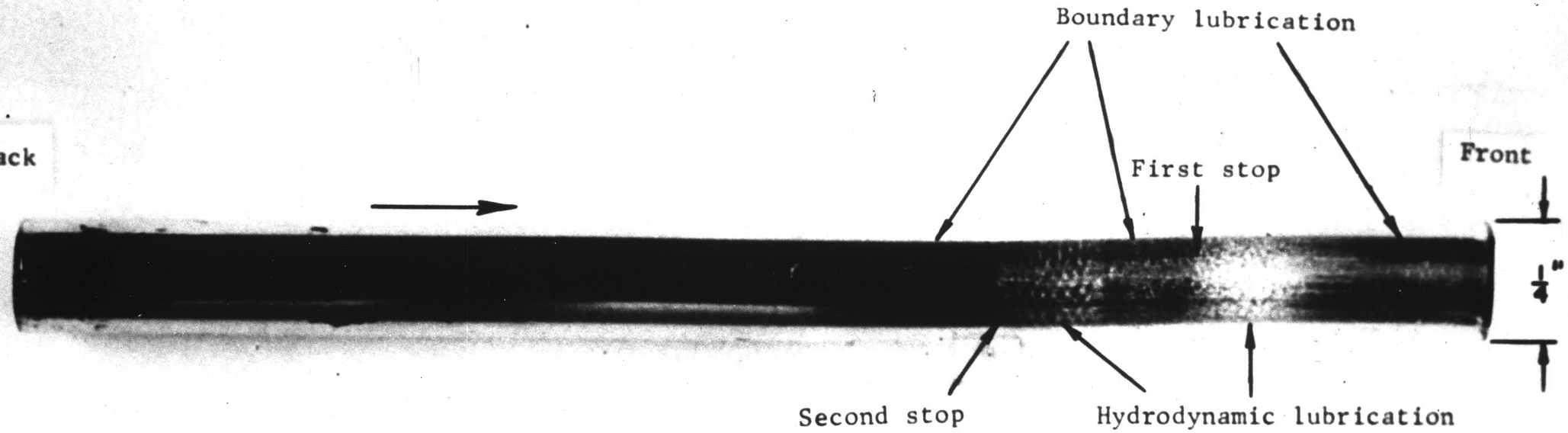

Fig. 17 Hydrostatically extruded billet

α = 15° Reduction = 36% Max. Pressure = 95,000 psi Min. Pressure = 71,000 psi

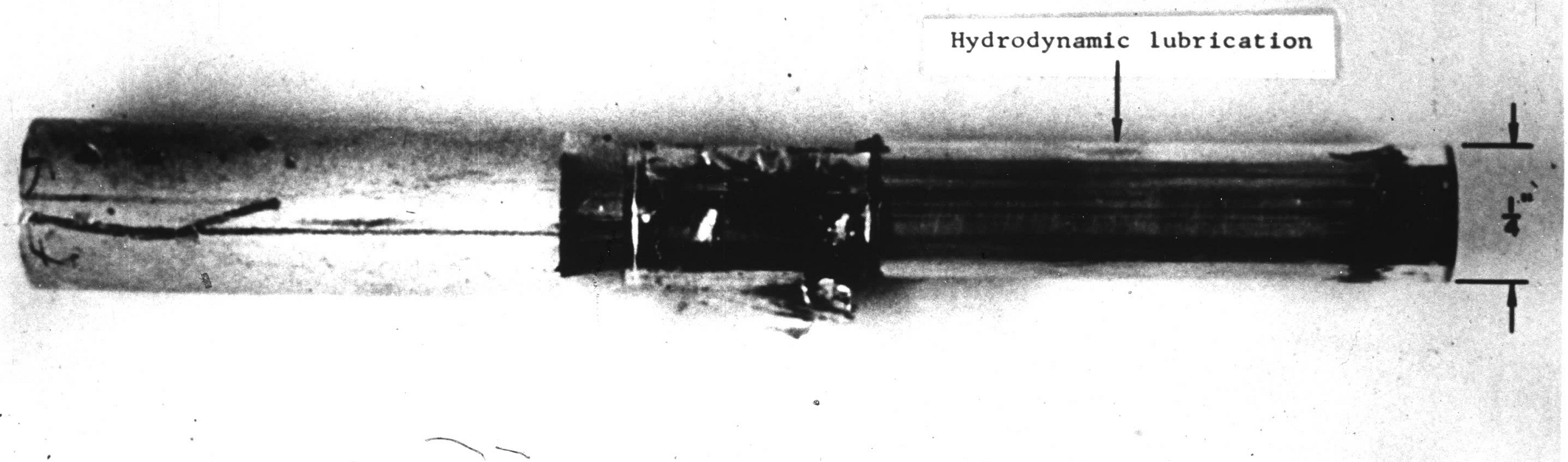

Fig. 18 Hydrostatically extruded billet

α = 22.5° Reduction = 36% Max. Pressure = 135,000 psi Min. Pressure = 83,000 psi

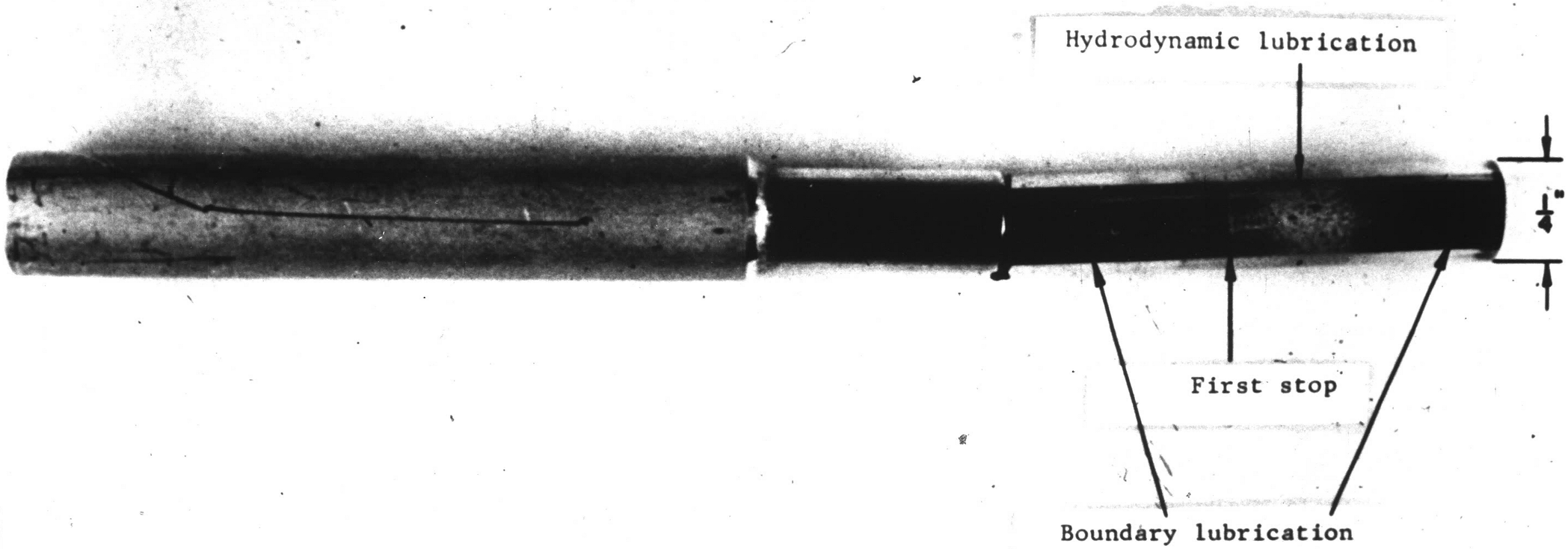

Fig. 19 Hydrostatically extruded billet

α = 30° Reduction = 36% Max. Pressure = 110,000 psi Min. Pressure = 94,000 psi

Boundary lubrication

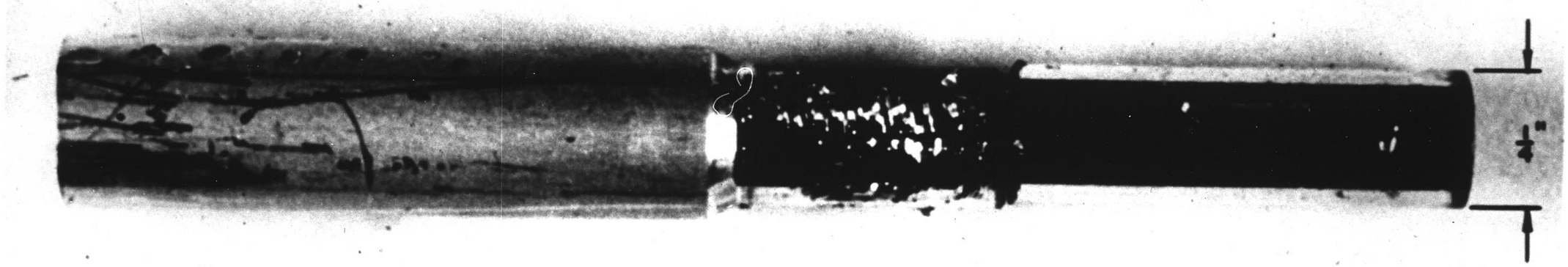

Fig. 20 Hydrostatically extruded billet

α = 40° Reduction = 36% Max. Pressure = 135,000 psi Min. Pressure 110,000 psi

Boundary lubrication

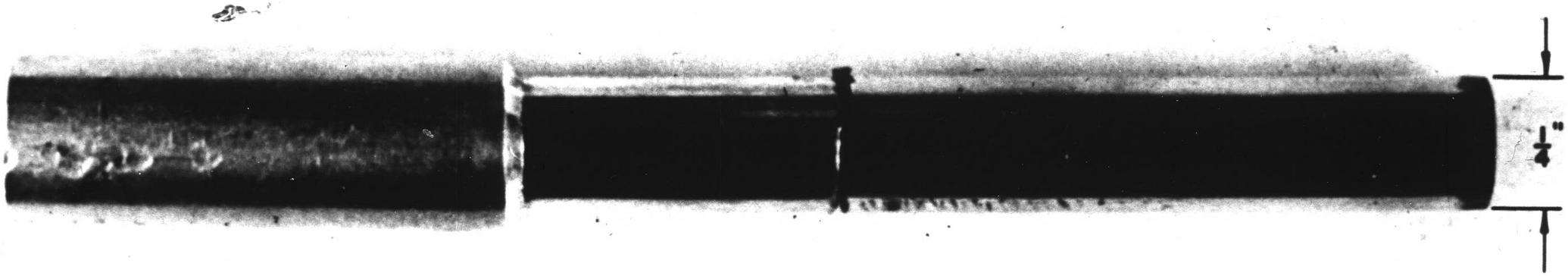

Fig. 21 Hydrostatically extruded billet

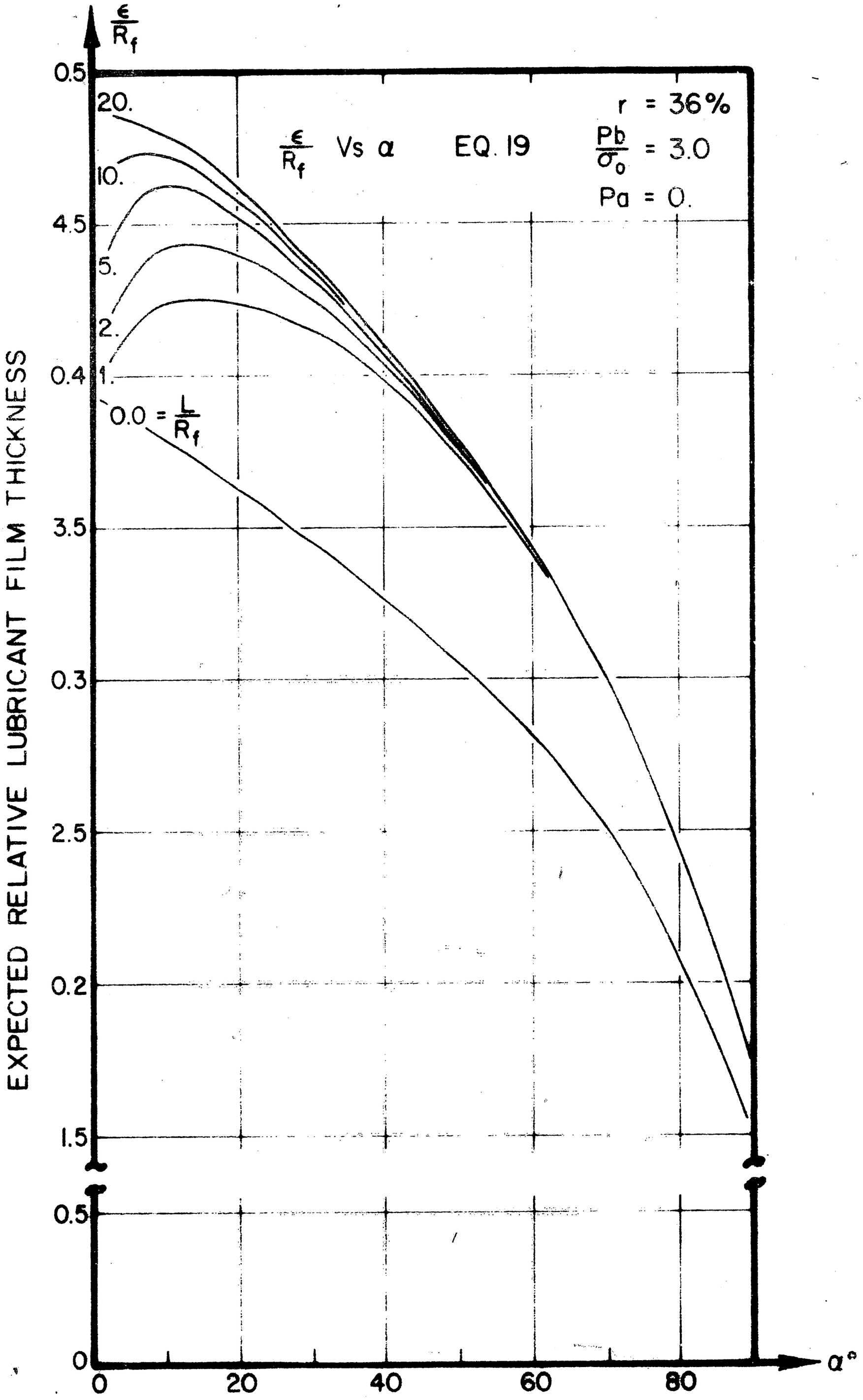

FIG. 22a EFFECT OF LAND AND DIE SEMI-CONE ANGLE ON THE EXPECTED RELATIVE LUBRICANT FILM THICKNESS DURING HYDROSTATIC EXTRUSION AND WIRE DRAWING.

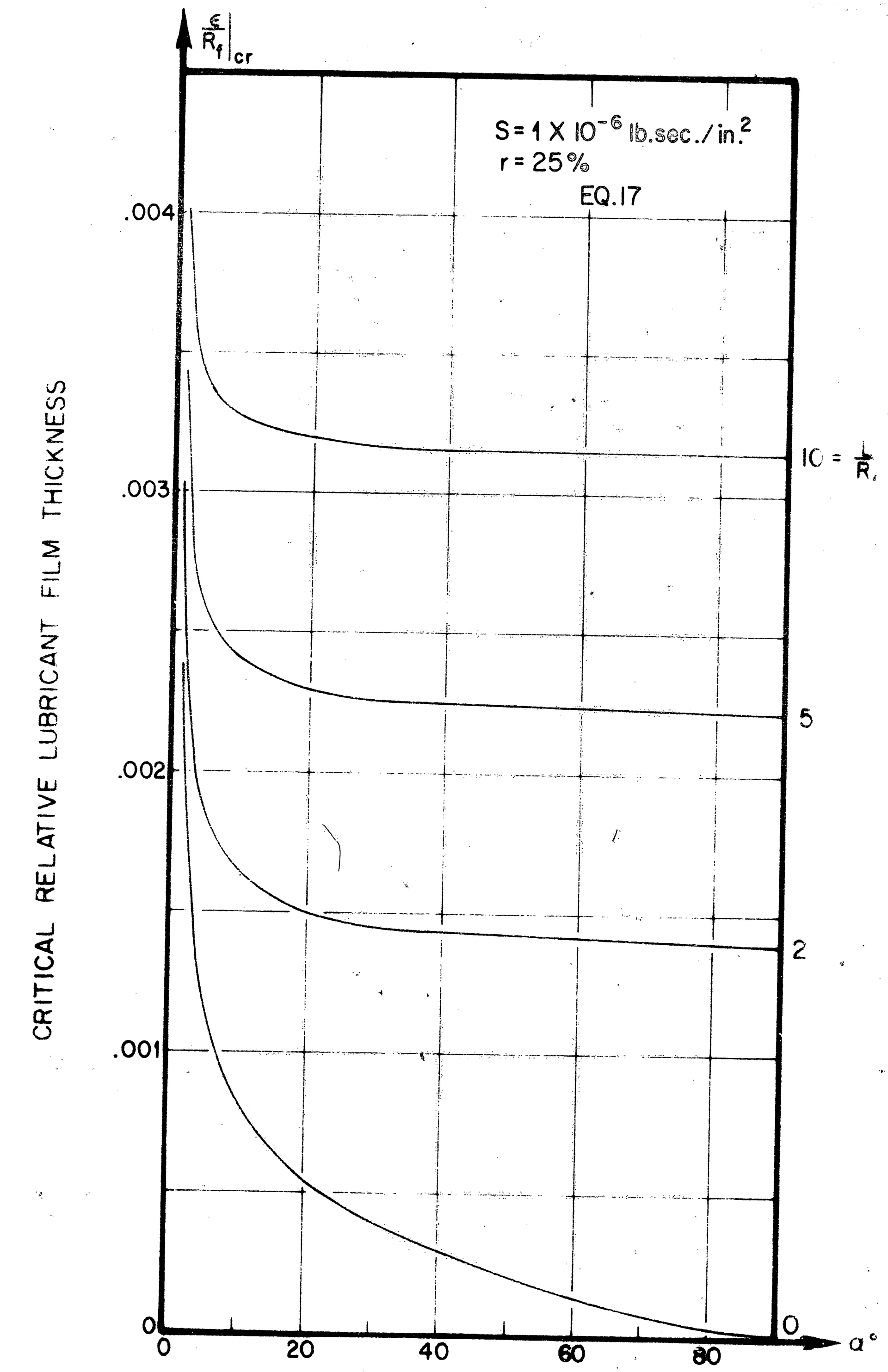

FIG. 22b EFFECT OF DIE LAND AND SEMI-CONE ANGLE ON THE CRITICAL RELATIVE LUBRICANT FILM THICKNESS IN WIRE DRAWING AND HYDROSTATIC EXTRUSION.

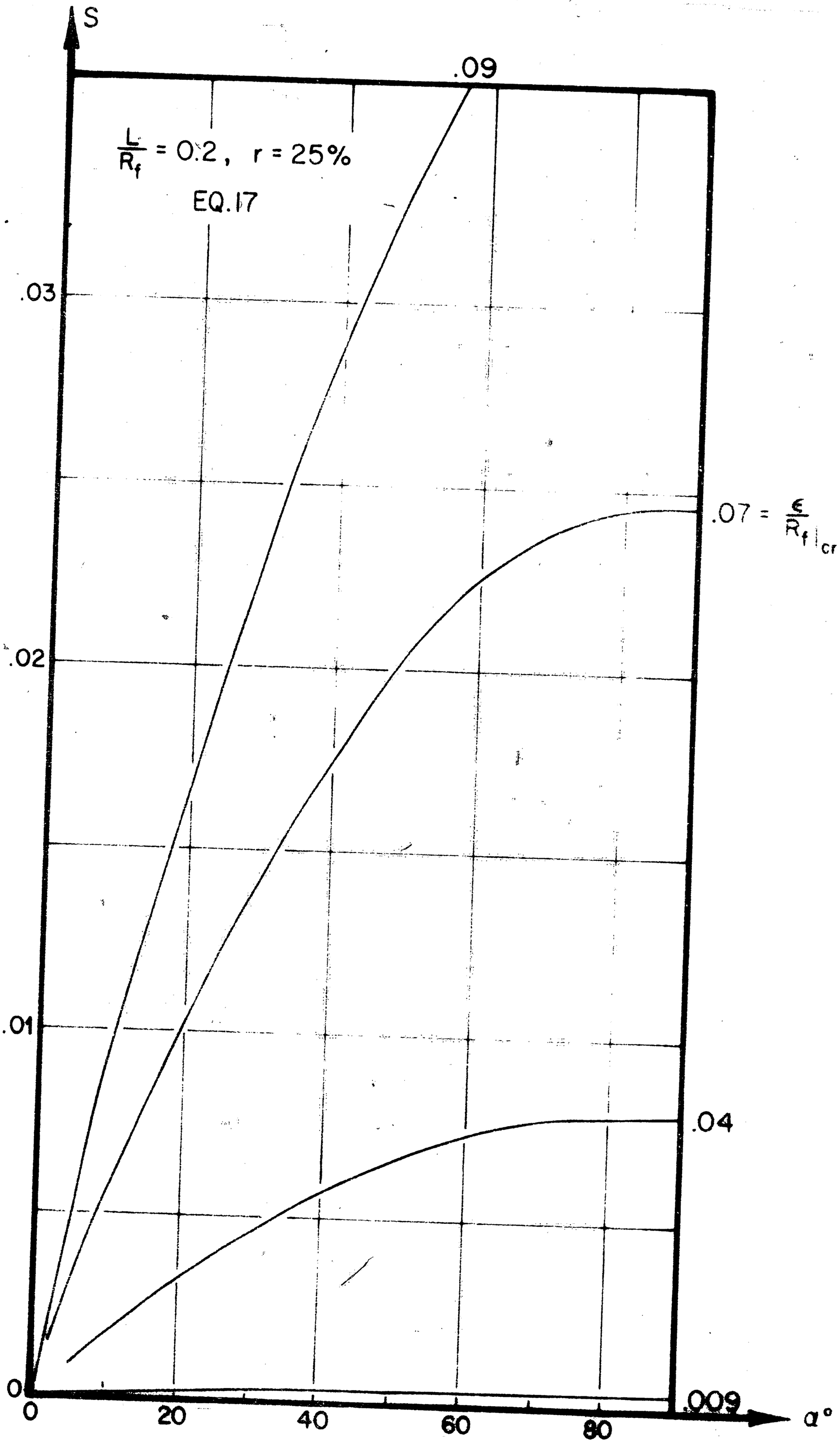

FIG. 22c EFFECT OF CRITICAL RELATIVE LUBRICANT FILM THICKNESS AND DIE SEMI-CONE ANGLE ON THE MODIFIED SOMMERFELD NUMBER IN WIRE DRAWING.

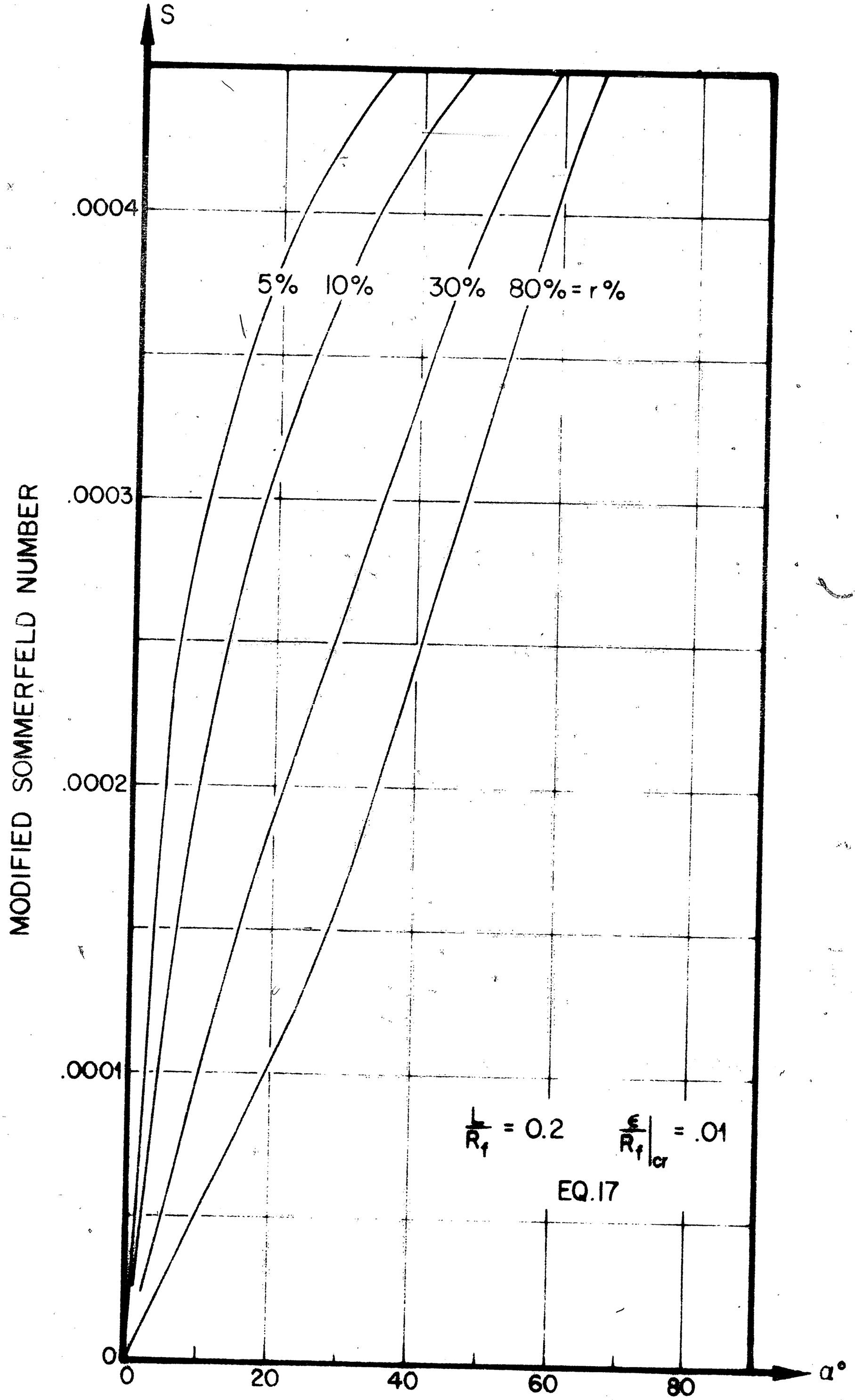

FIG. 22d EFFECT OF PERCENT REDUCTION AND DIE SEMI-CONE ANGLE ON MODIFIED SOMMERFELD NUMBER IN WIRE DRAWING.

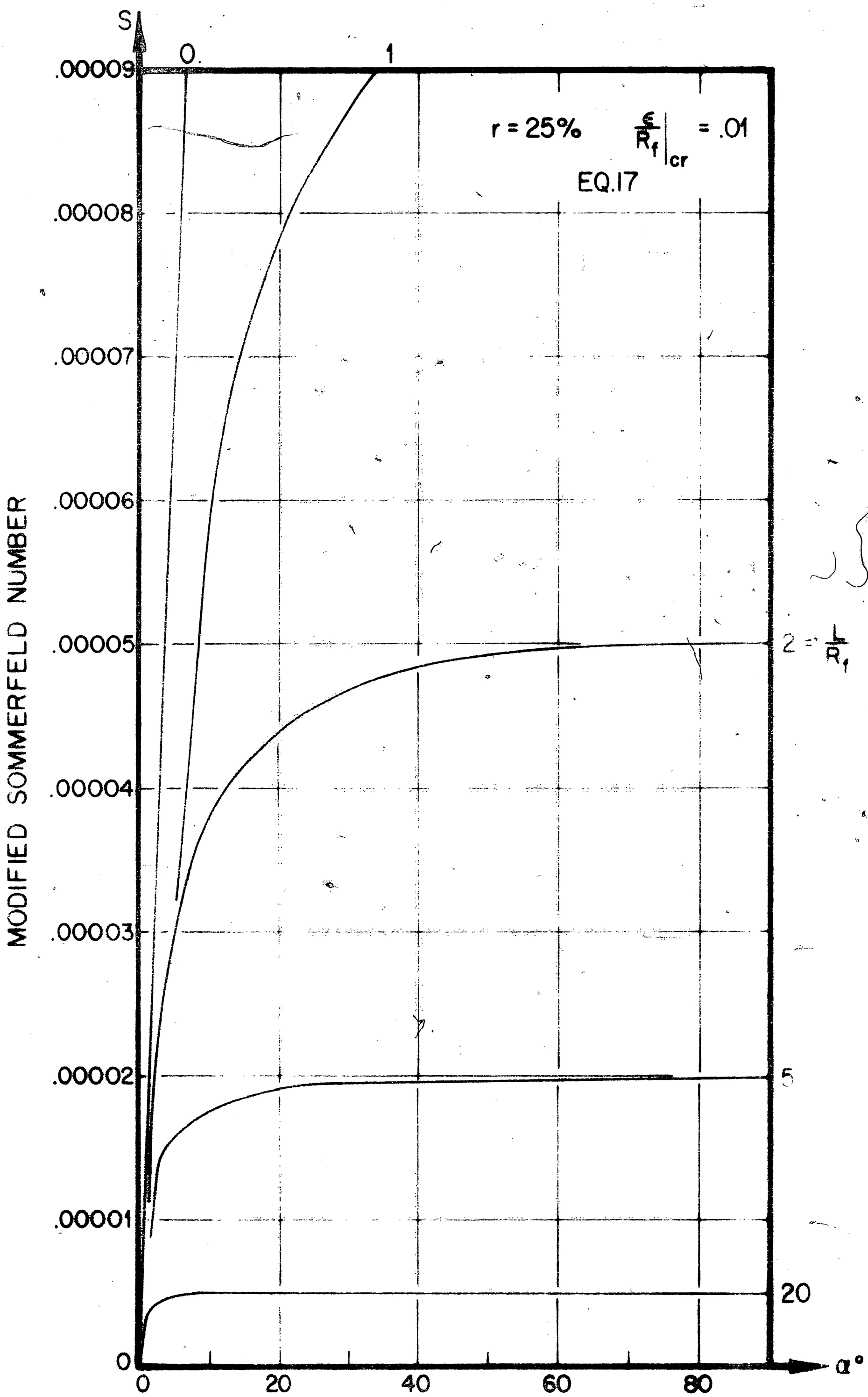

FIG.22e EFFECT OF DIE LAND AND DIE SEMI-CONE ANGLE ON MODIFIED SOMMERFELD NUMBER IN WIRE DRAWING

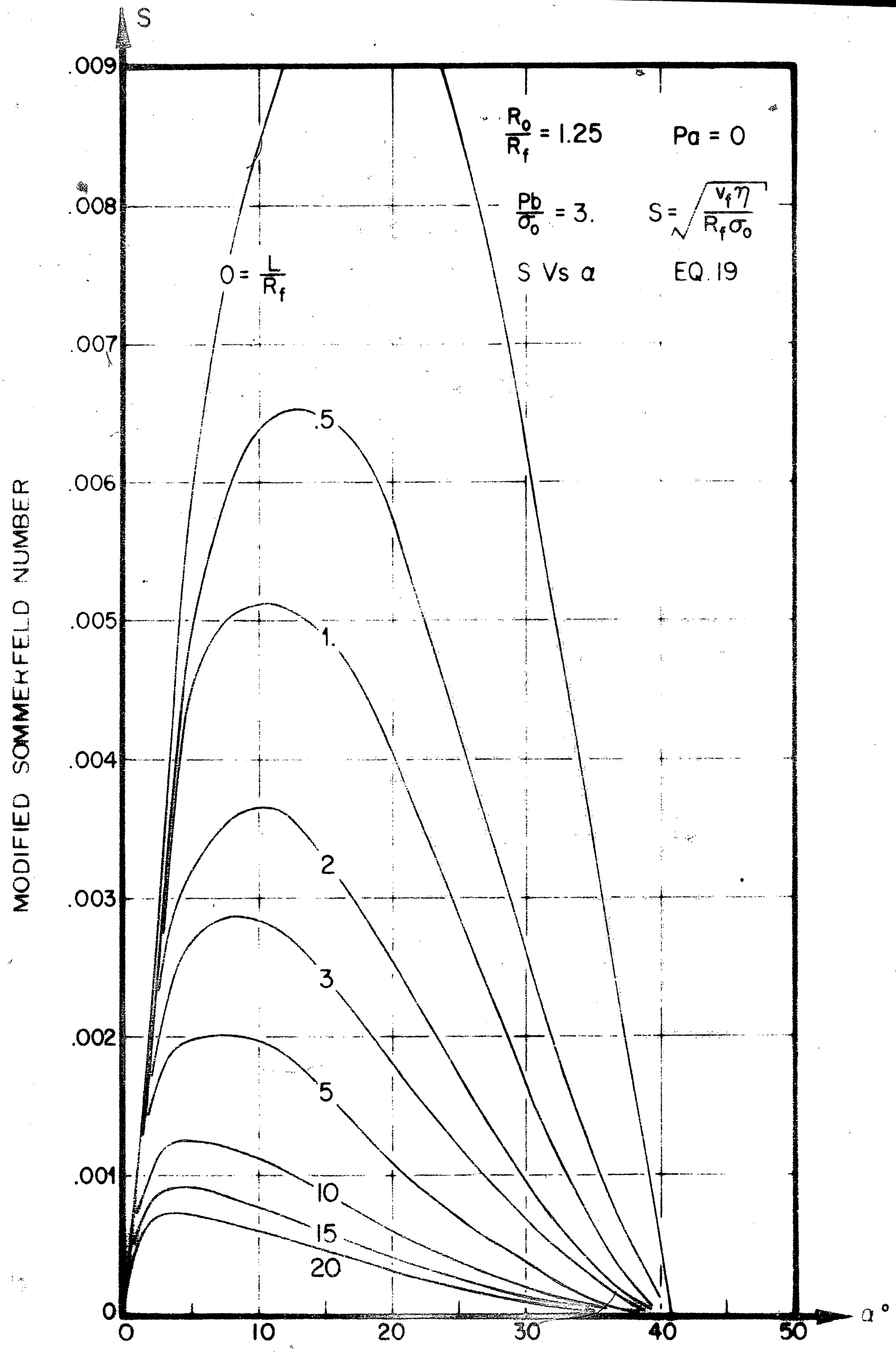

FIG. 23 EFFECT OF DIE LAND AND DIE SEMI-CONE ANGLE ON MODIFIED SOMMERFELD NUMBER DURING HYDROSTATIC EXTRUSION.

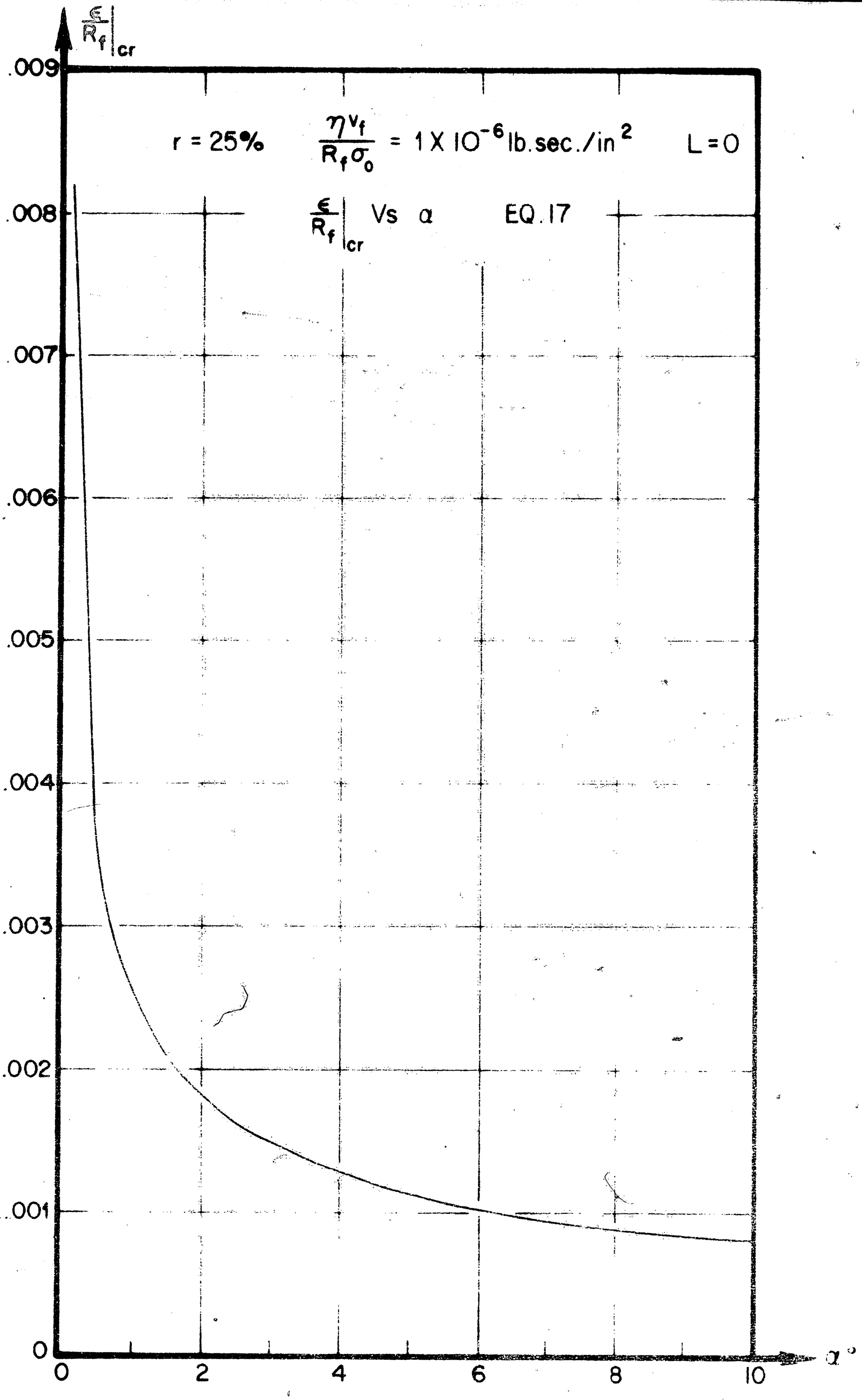

FIG. 24 EFFECT OF DIE SEMI-CONE ANGLE ON RELATIVE LUBRICANT FILM THICKNESS DURING HYDROSTATIC EXTRUSION AND WIRE DRAWING.

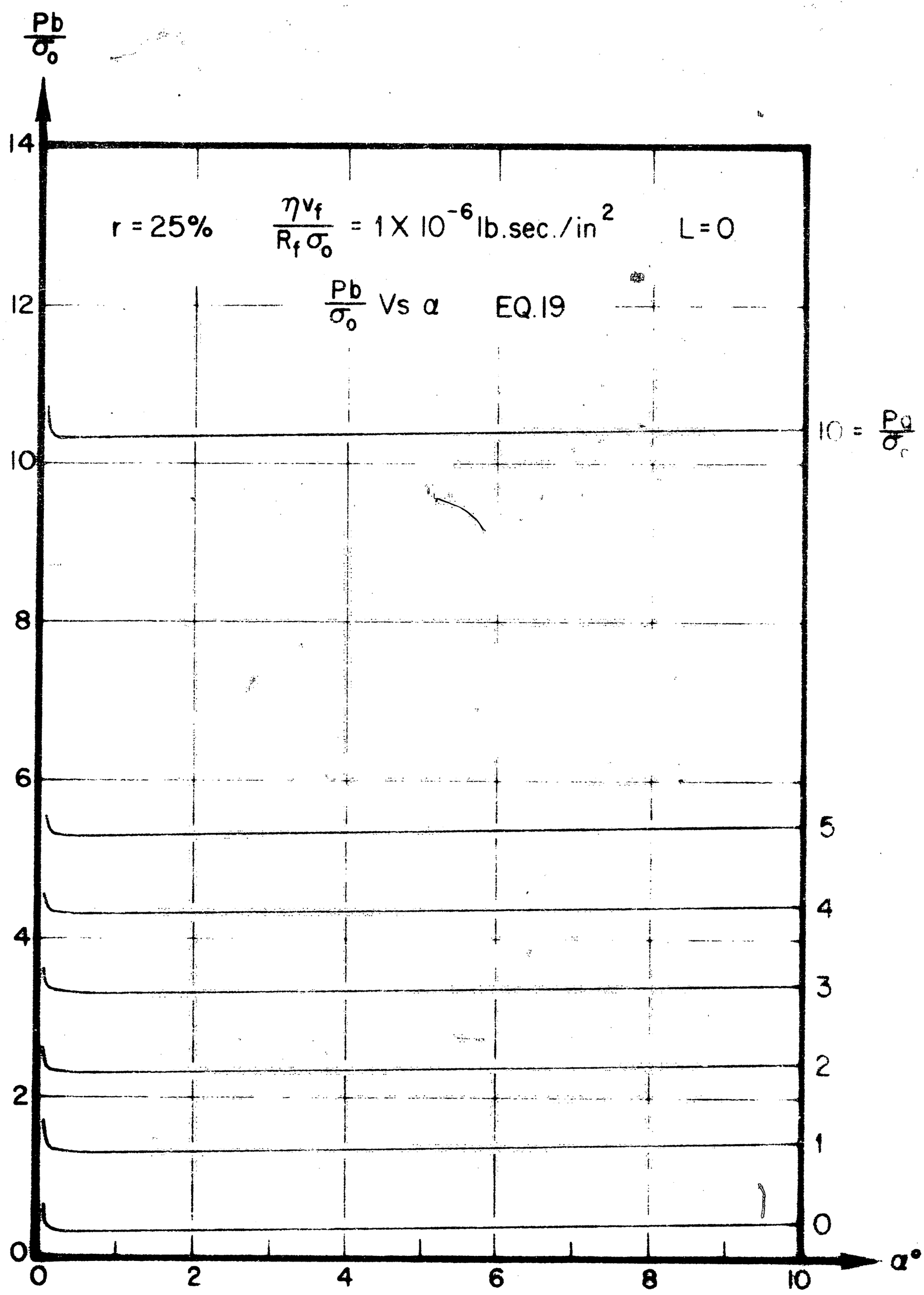

FIG. 25 EFFECT OF RECEIVER RELATIVE PRESSURE AND DIE SEMI-CONE ANGLE ON RELATIVE EXTRUSION PRESSURE DURING HYDROSTATIC EXTRUSION.

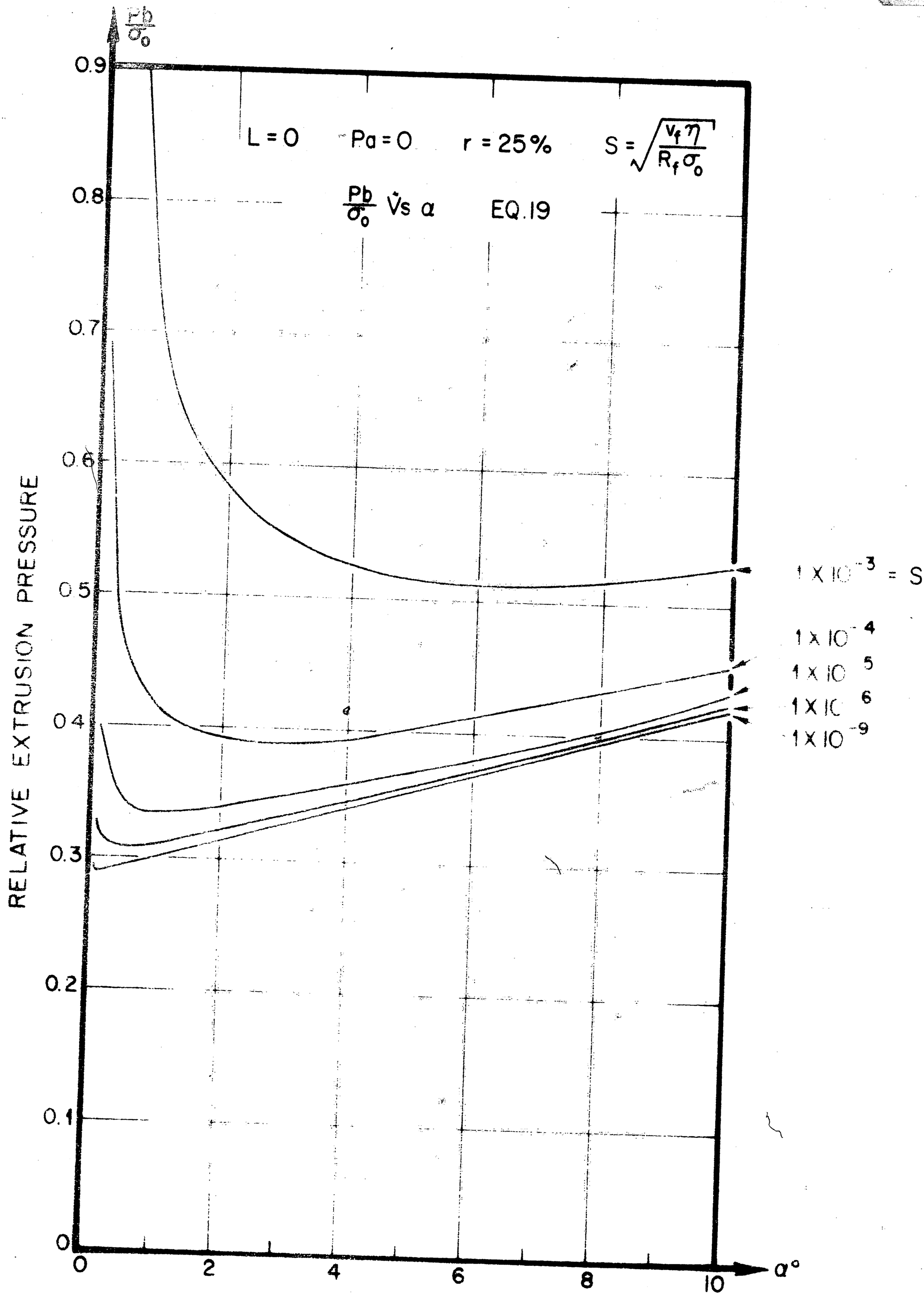

FIG. 26 EFFECT OF MODIFIED SOMMERFELD NUMBER AND DIE SEMI-CONE ANGLE ON RELATIVE EXTRUSION PRESSURE DURING HYDROSTATIC EXTRUSION.

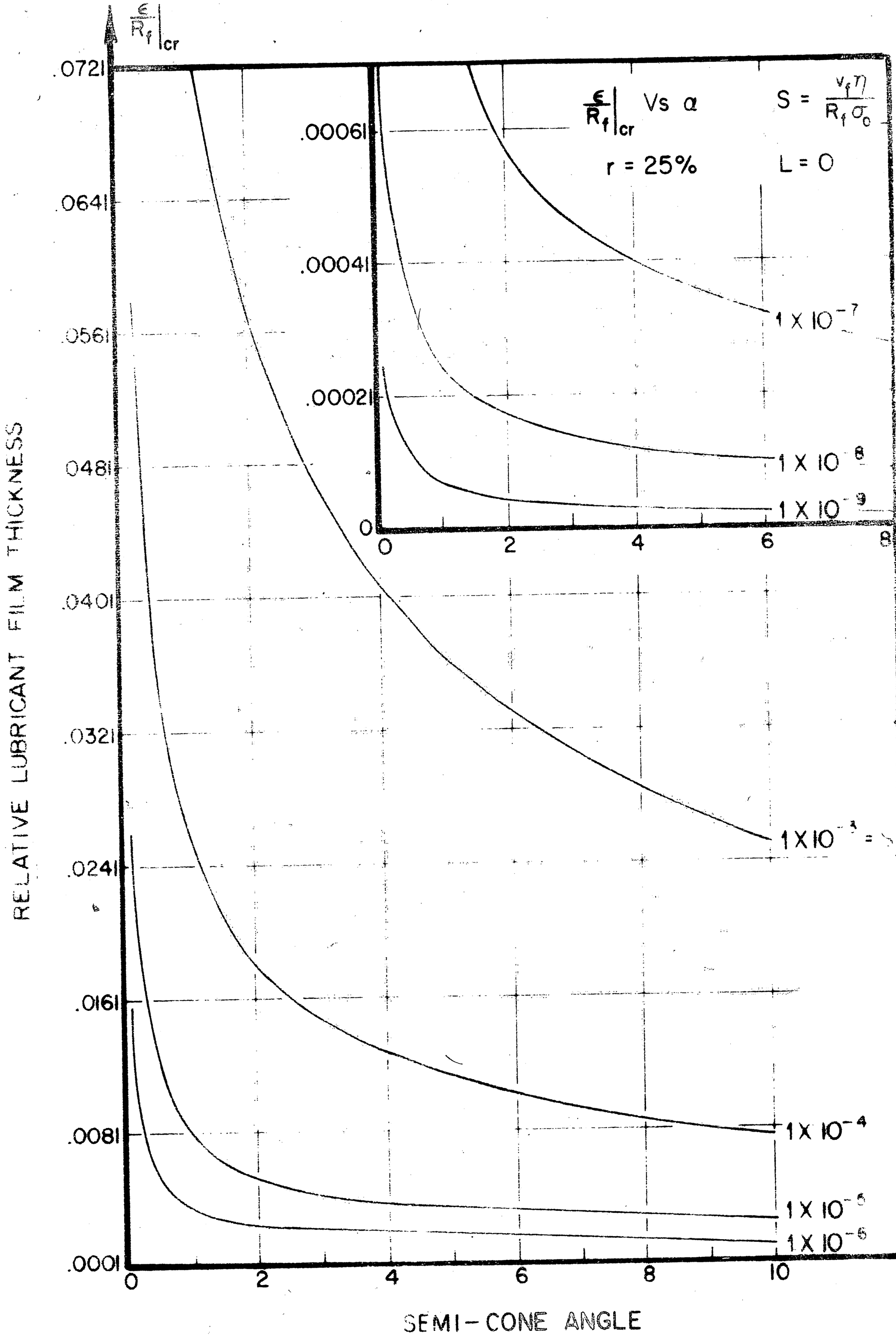

FIG. 27 EFFECT OF MODIFIED SOMMERFELD NUMBER AND DIE SEMI-CONE ANGLE ON RELATIVE LUBRICANT FILM THICKNESS DURING HYDROSTATIC EXTRUSION AND WIRE DRAWING

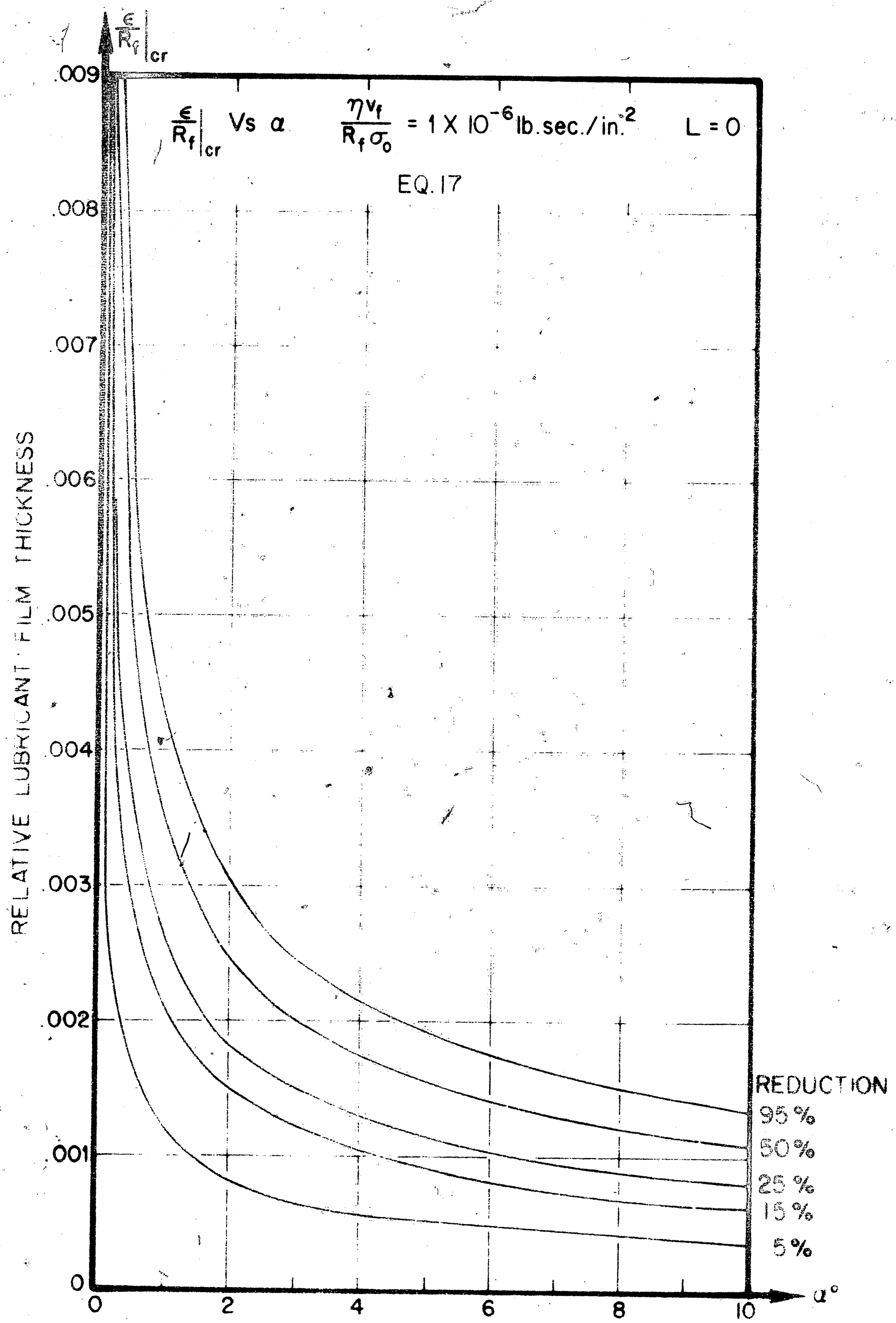

FIG. 28 EFFECT OF PERCENT REDUCTION AND DIE SEMI-CONE ANGLE ON RELATIVE LUBRICANT FILM THICKNESS DURING HYDROSTATIC EXTRUSION AND WIRE DRAWING.

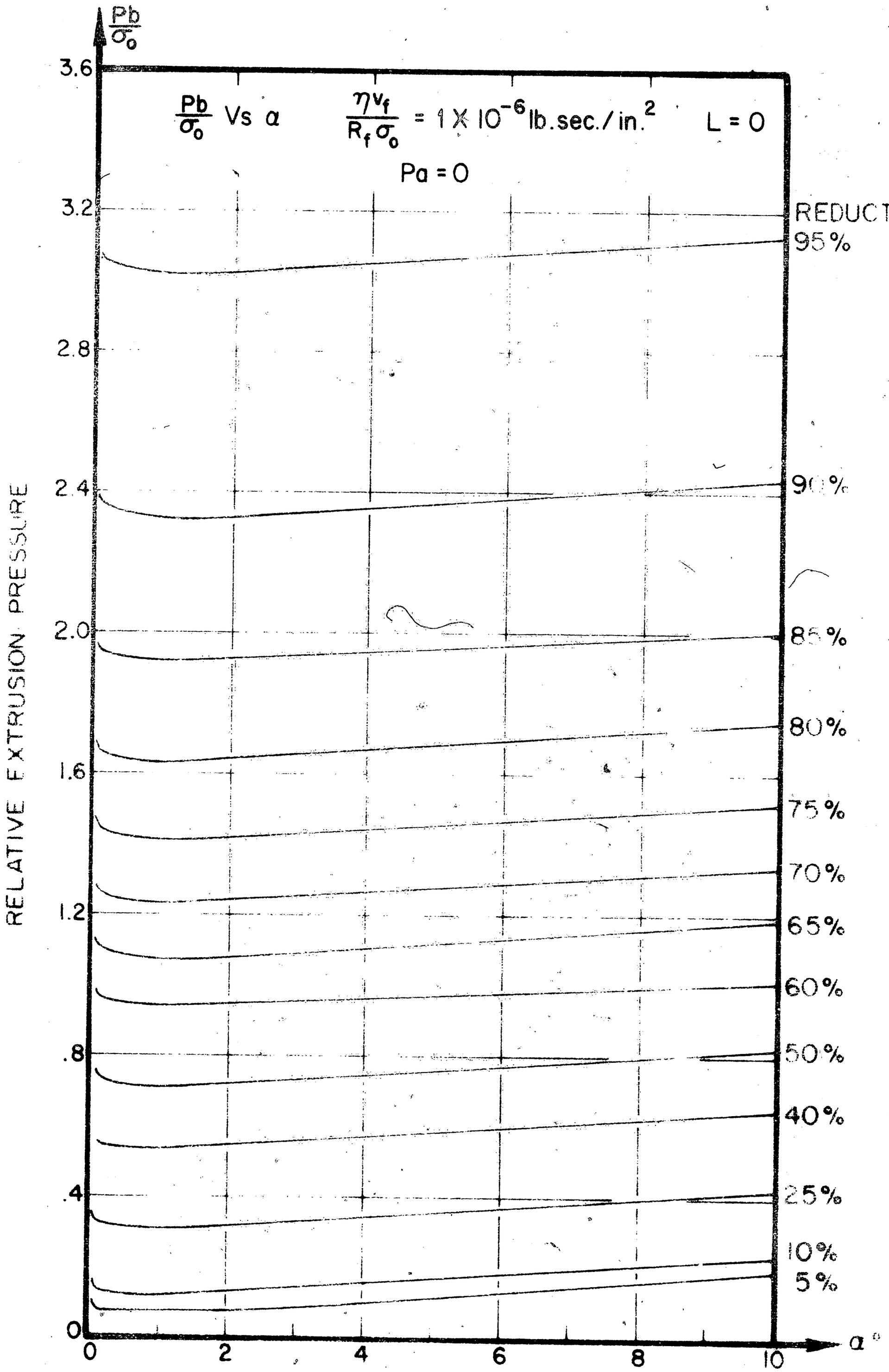

FIG. 29 EFFECT OF PERCENT REDUCTION AND DIE SEMI-CONE ANGLE ON RELATIVE EXTRUSION PRESSURE DURING HYDROSTATIC EXTRUSION.

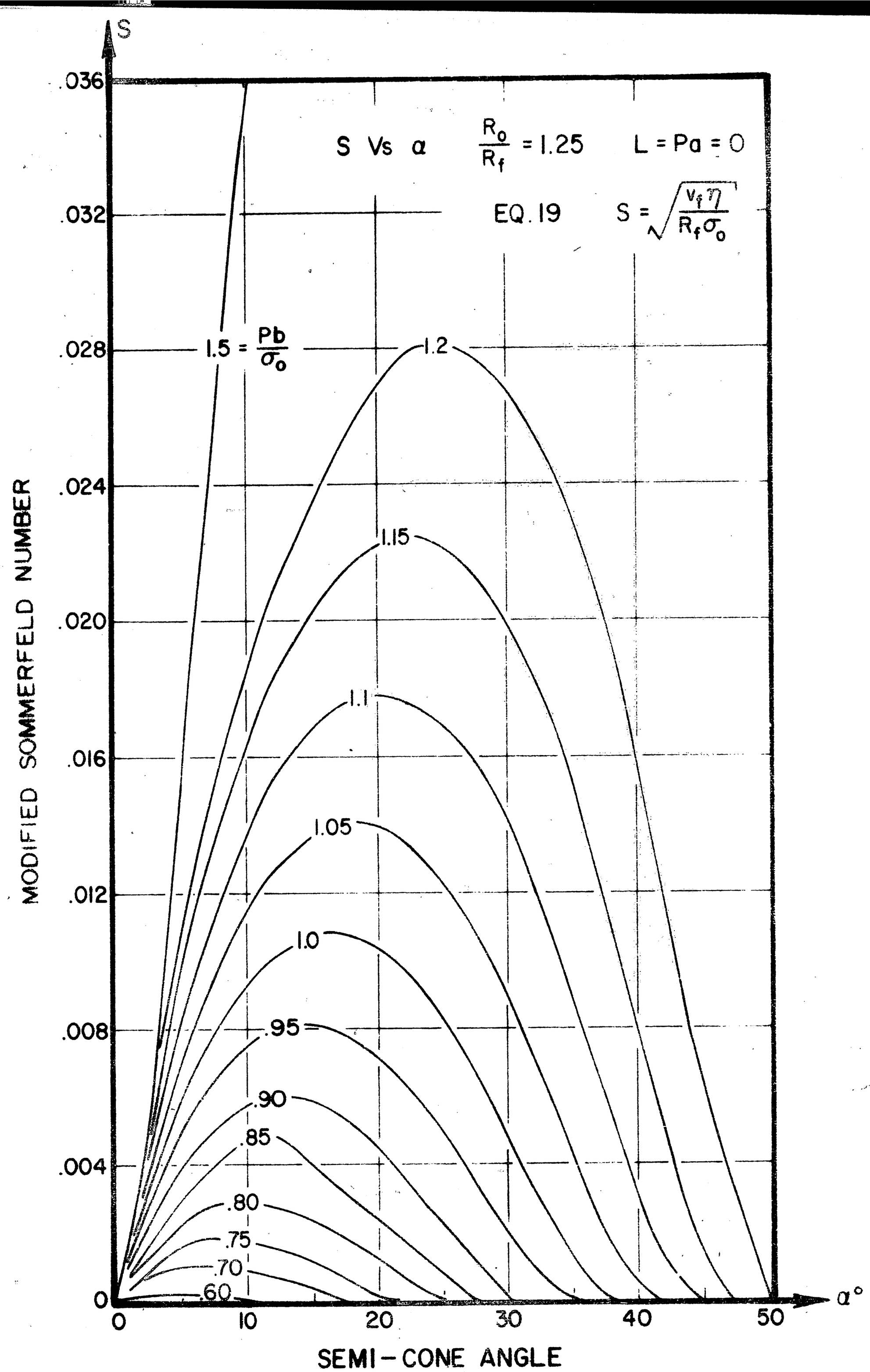

FIG. 30 EFFECT OF RELATIVE EXTRUSION PRESSURE AND DIE SEMI-CONE ANGLE ON MODIFIED SOMMERFELD NUMBER DURING HYDROSTATIC EXTRUSION.

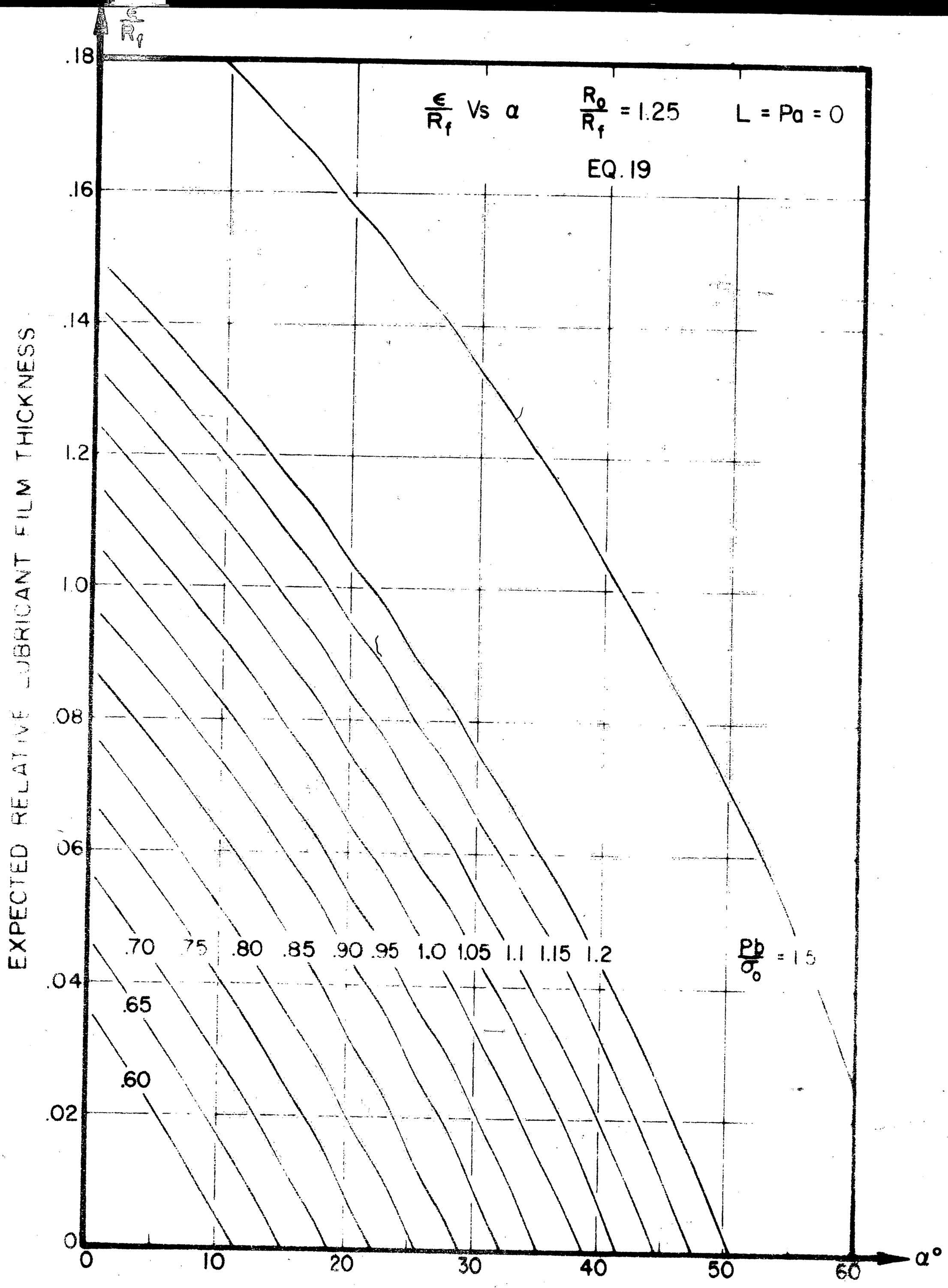

FIG. 31 EFFECT OF RELATIVE EXTRUSION PRESSURE AND DIE SEMI-CONE ANGLE ON RELATIVE LUBRICANT FILM THICKNESS DURING HYDROSTATIC EXTRUSION.

REFERENCES

1. Wistreich, J. G., "Investigation of the Mechanics of Wire Drawing," Proceedings of Institute of Mechanical Engineers, Vol. 169, 1955, pp. 654-678.

2. Avitzur, B., "Analysis of Wire Drawing and Extrusion Through Conical Dies of Large Cone Angles," Trans. ASME, Engineering for Industry, Series B, Vol. 86, Nov. 1964, pp. 305-316.

3. Avitzur, B., "Analysis of Wire Drawing and Extrusion Through Conical Dies of Small Cone Angles," Trans. ASME, Engineering for Industry, Series B, Vol. 85, Feb. 1963, pp. 89-96.

4. Wistreich, J. G., "The Fundamentals of Wire Drawing," Metallurgical Reviews, Vol. 3, 1958, pp. 97-142.

5. Avitzur, B., "Flow Characteristics Through Conical Converging Dies," Trans. ASME, Engineering for Industry, Series B, Vol. 88, Nov. 1966, pp. 410-420.

6. Pearson and Parkins, "The Extrusion of Metals," John Wiley and Sons, Inc., New York, 1960.

7. Avitzur, B., "Analysis of Metal Extrusion," Trans. ASME, Engineering for Industry, Series B., Vol. 87, No. 1, Feb. 1965, pp. 57-70.

8. Frisch, J. and Thomsen, E. G., "The Effect of Process Variables on Extrusion Pressure of Lead," Transactions of ASME, Journal of Engineering for Industry, August 1959, pp. 207-216.

9. Bishop, J. F. W., "The Theory of Extrusion," Metallurgical Reviews, Vol. 2, 1957, pp. 361-390.

10. Pugh, H. Ll. D., The Cold Extrusion of Steel, Bullied Memorial Lectures 1965, Vol. IIIA, University of Nottingham.

11. Treco, R. M., "Theoretical and Experimental Analysis of Extrusion Process for Metals," Transactions of ASME, Vol. 55, 1962, pp. 697-718.

12. Frisch, J. and Thomsen, E. G., "An Experimental Study of Metal Extrusions at Various Strain Rates," Transactions of ASME, May 1954, pp. 599-606.

13. Everhart, J. L., "Impact and Cold Extrusion of Metals," Chemical Publishing Co., Inc., New York, 1964.

14. Fioretino, R. J., Sabroff, A. M., and Boulger, F. W., "Advances in Hydrostatic Extrusion," The Tool and Manufacturing Engineer, August 1963, pp. 77-83.

15. Fluid to Fluid Extrusion of Materials, The Engineer, Feb. 8, 1963, pp. 290-291.

16. Pugh, H. Ll. D., "Hydrostatic Extrusion," Bullied Memorial Lectures, 1965, Vol. IIIB, University of Nottingham.

17. Avitzur, B. and Sortais, H. C., "Experimental Study of Hydrostatic Extrusion," Journal of Basic Engineering, Transactions of ASME, Series D, Vol. 88, No. 3, Sept. 1966, pp. 658-668.

18. Avitzur, B., "Hydrostatic Extrusion," Journal of Engineering for Industry Transactions of ASME, Series B, Vol. 87, 1965, pp. 487-494.

19. Bobrowsky, A. and Stack, E. A., "Fluid Extrusion As a Drawing Process," Nature, May 4, 1963.

20. Bowden, F. P. and Tabor, D., "Friction and Lubrication," Methuen and Co., Ltd., London, John Wiley and Sons, Inc., New York, 1956.

21. Stribeck, R., "Die Wesentlichen Eigenschaften Der Gleit-und Rollenlager," Zeitschrift des Vereines Deutscher Ingenieure, No. 36, Band XXXXVI, Sept. 6 1902, pp. 1341-1348.

22. D.M.I.C. Report 226, July 7, 1966, Defence Materials Information Centre, Battelle Memorial Institute, Columbus, Ohio, 43201.

23. Davis, W. M., "Friction and Lubrication," The Lubrication Publishing Co., Pittsburgh, 1904.

24. Sommerfeld, A., "Mechanics of Deformable Bodies," Academic Press Inc., Publishers, 1950.

25. Roberts, R. W. and Owens, R. S., "A Chemical Approach to Lubrication," General Electric Co., Report No. 66-C-091, March 1966.

26. Hersey, M. D., "Theory of Lubrication," John Wiley and Sons, Inc., N. Y., 1936.

27. Clower, J. I., "Lubricants and Lubrication," Mc-Graw Hill Book Co., New York and London, 1939.

28. Tipei, N., "Theory of Lubrication," Stanford University Press, Stanford, California, 1962.

29. Pinkus and Sternlicht, "Theory of Hydrodynamic Lubrication," Mc-Graw Hill Book Co., Inc., New York, 1961.

30. Hillier, M. J., "A Hydrodynamic Model of Hydrostatic Extrusion," International Journal of Production Research, Vol. 5, pp. 171-181, 1967.

31. Christopherson, D. G., "Promotion of Fluid Lubrication in Wire Drawing," Proceedings of the ASME, Vol. 169, 1955, p. 643.

32. Sturgeon, G. M. and Tattersal, G. H., "Thick Film Lubrication in Wire Drawing," The Wire Industry, 26 (312), 1183-1186, Dec. 1959.

33. Moseev, V. F. and Korostilim, A. A., "New Method of Feeding Lubricant to the Deformed Zone in Wire Drawing," STAL in English, 3, pp. 237-239, March 1962.

34. Butler, L. H., "A Method for Continuous Wire Drawing Aided by Externally Generated Hydrostatic Oil Pressure," Journal of Institute for Metals, Vol. 93, pp. 123-125, (1964-65).

35. Avitzur, B., "Metal Forming-Processes and Analysis," Book to be published by McGraw Hill Book Co., New York.

36. Prager, W. and Hodge, P. G., Theory of Perfectly Plastic Solids, John Wiley and Sons, Inc., New York, 1951.

37. Naden, J. W. R., "The Extrusion of Steel Tubes," Journal of The Iron and Steel Institute, Vol. 193, November 1959, pp. 278-284.

38. Ling, F. F., Whiteley, R. L., Ku, P. M., Peterson, M. B. (Editors) "Friction and Lubrication in Metal Processing," The American Society of Mechanical Engineers, 1966.

VITA

Arumugam Manoharan, son of V. S. Arumugam Nadar of Madras, India, was born in Virudhunagar, Madras State, India on November 8, 1940. He attended Thangappa Nadar Elementary School in Madras and obtained his secondary education at Christian College School, Madras, where he graduated in June 1956. He then entered Sir Theagaraya College, Madras, for the Pre-University course (1956-'57). In the Fall of 1957 he joined P. S. G. College of Technology, Coimbatore, India and was awarded a Bachelor of Engineering degree in Mechanical Engineering in June, 1962. Upon receipt of this degree, the author was employed as an Engineering Trainee by Tube Products of India, Madras-54, India. The following year he was promoted to Engineer in one of the production shops of the company. In the spring of 1966, he entered the Graduate School of Lehigh University, Bethlehem, Pa. and in the fall of the same year, became a research assistant on a project sponsored by National Science Foundation.

He is a member of the American Society of Mechanical Engineers.

He is married and has a daughter.